Catheterized bladder environment induces *Candida albicans* hyphal formation and promotes colonization and persistence through Als1.

Alyssa Ann La Bella[1], Marissa Jeme Andersen[1], Nicholas C. Gervais[2], Jonathan Jesus Molina[1], Alex Molesan[1], Peter V. Stuckey[1], Lauren Wensing[2], Rebecca S. Shapiro[2], Felipe Hiram Santiago-Tirado[1]*, & Ana Lidia Flores-Mireles[1]*

[1]Department of Biological Sciences, University of Notre Dame, Notre Dame, IN, USA
[2]Department of Molecular and Cellular Biology, University of Guelph, Guelph, ON, Canada.

*Address correspondence to Ana Lidia Flores-Mireles (ALFM), afloresm@nd.edu,
and Felipe Hiram Santiago-Tirado(FHST), fsantiago@nd.edu

Mailing address: 351 Galvin Life Science Center, Notre Dame, IN 46556, USA. Phone: (574) 631-4964 (ALFM) and (574) 631-4096 (FHST).

Short title: Catheterized bladder environment induces *Candida* virulent programming

Key words: *C. albicans*; CAUTI; UTI; Efg1; Als1; filamentation; hyphae; biofilm; urine; bladder; catheter; candiduria; fungi; fibrinogen-binding protein.

ABSTRACT

When *Candida* is found in the urine, physicians face the dilemma to treat or not, since its presence could represent commensalism or infection, resulting in inappropriate management. *Candida spp.,* specifically *Candida albicans,* are the second most common cause of catheter-associated urinary tract infections (CAUTIs). Yet, the cellular and molecular details of *C. albicans* CAUTI are poorly understood. With the steady increase in catheter usage, combined with fungal infection mismanagement and treatment challenges, this question is of utmost public health importance. Here, for the first time, we characterized fungal mechanisms during CAUTI, finding that the catheterized bladder environment triggers *Candida* virulent programing, inducing Efg1-dependent hyphal morphogenesis, required for CAUTI establishment. Moreover, Als1, an Efg1-downstream effector, is necessary for *in vitro* and *in vivo* fibrinogen-biofilm formation and Als1 expression levels were crucial for fungal persistence during CAUTI. These findings unveil the mechanisms for fungal CAUTIs and identify potential treatment targets.

INTRODUCTION

Candiduria (*Candida* in urine) is one of the most problematic issues in patient management. This problem is due to the lack of evidence-based information on the pathogenicity of *Candida species* (spp.), as it is unclear whether candiduria results from contamination, commensal colonization or invasive infection, representing a conundrum for the physician [1-3]. This is further complicated by the shortfalls of defined laboratory criteria for diagnosis of fungal urinary tract infections (UTI) as the studies are standardized by bacterial UTI [1]. As *Candida spp.* are becoming increasingly resistant to antifungal therapy [4, 5], the management of this fungal pathogen is a major challenge for the medical community [6].

Candiduria is a common nosocomial infection, especially for those in intensive care units (ICU) [7]. It is primarily associated with patients with predisposing factors including diabetes mellitus, genitourinary structural abnormalities, diminished renal function, renal transplantations, metabolic abnormalities, and indwelling urinary tract catheters or devices [8]. However, most of the fungal UTIs occur in hospitalized patients with indwelling bladder catheters [7]. The 2016 National Healthcare Safety Network review found that *Candida spp.*, specifically *C. albicans*, have become the second most prevalent uropathogen causing 17.8% of catheter associated urinary tract infections (CAUTIs) [9]. CAUTIs are the most common nosocomial infection with more than 150 million individuals acquiring these infections per year [10]. The use of catheters and subsequent infections are not limited to hospital-care settings, in nursing homes, 11.9% of residents use indwelling catheters [11], and ~50% of nursing home residents with indwelling urinary catheters will experience symptomatic CAUTIs [12]. Despite *Candida spp*. prevalence in CAUTIs, there are no studies available regarding the pathogenesis of *Candida spp*. in the catheterized bladder and the role of host and fungal factors that promote *Candida* pathogenesis during CAUTIs remain unclear [9, 13].

C. albicans can grow in yeast, pseudohyphal, and hyphal morphologies [14, 15] and hyphal formation and hyphae-specific gene expression are critical for virulence, invasion, and immune evasion, resulting in tissue damage and invasive infections [16]. *C. albicans* can transition to hyphal growth via numerous environmental signals including, serum, neutral pH, and CO_2, and is controlled by master transcriptional regulators such as Enhanced filamentous growth protein 1 (Efg1) [17].

Switching between yeast and hyphal forms is essential for pathogenesis and biofilm formation, which is a key fungal virulence trait [15-19]. Biofilm formation initiates with the adherence of yeast cells to a surface, forming microcolonies followed by proliferation of hyphae and pseudohyphae [16]. Biofilm maturation occurs when the hyphal scaffold is encased in an extracellular polysaccharide matrix [20] and the final step in biofilm formation involves dispersion of non-adherent yeast cells for biofilm establishment in the surrounding environment [16]. *Candida* biofilms pose a serious threat to the host as biofilms are more resistant to antifungal therapy and can evade protection from host defenses [20]. New antifungal treatments, such as the echinocandins, that target the β-1,3 glucan component of the cell wall have proven to successfully prevent *C. albicans* biofilms [21]; unfortunately, recently echinocandin-resistant *Candida spp.* are emerging [22].

C. albicans colonization and overgrowth in different infection models have been associated with dysbiosis in the host environment such as alterations in host immunity, stress, and resident microbiota [18]. Urinary catheterization disrupts the bladder homeostasis, mechanically compromising the integrity of the urothelium, inducing inflammation, interfering with normal micturition (voiding), and disrupting host defenses in the bladder [23-25]. The inflammation response caused by catheterization exposes cryptic epithelial receptors or recruits host factors that can be recognized by the pathogen, enabling microbial colonization, multiplication, and persistence within the urinary tract [23-25]. One of these factors is fibrinogen (Fg), which is released into the bladder to heal damaged tissue and prevent bleeding due to catheter-induced inflammation in both mice and humans [26, 27]. However, due to the constant mechanical damage caused by the urinary catheter, Fg accumulates in the bladder and deposits onto the catheter, where it is exploited by uropathogens [26-29]. Consistently, in an *ex vivo* study, we showed that a *C. albicans* CAUTI isolate binds to urinary catheters via Fg [27]. This strongly suggests that urine is inducing changes in the expressed Fg-binding adhesins, prompting us to study this Fg-fungal interaction in more detail.

Here, we characterized five *C. albicans* clinical and laboratory strains' growth and morphology in urine, biofilm formation, and capability to cause CAUTI. We found that urine supported *C. albicans* growth, activated virulence programming by inducing hyphal morphology and enhanced Fg-dependent biofilm formation mediated by the transcriptional regulator Efg1. Furthermore, we found that the catheterized-induced inflammation is necessary for fungal colonization of the urinary tract and further demonstrated that Efg1-dependent hyphal formation is critical for CAUTI establishment. Importantly, we identified that the Efg1-downstream adhesin, Als1, is important for mediating Fg-fungal interaction *in vitro* and *in vivo* and its expression is crucial for fungal CAUTI. This suggests development of therapies that target the Als1-mediated fungal-Fg interaction could potentially treat *C. albicans* CAUTIs.

RESULTS

C. albicans survives and grows in urine.

C. albicans is able to infect a wide range of human sites including oropharyngeal, gastrointestinal, intra-abdominal, skin, genital, and urinary tract, demonstrating its plasticity to survive and replicate in different host environments [10, 17, 18, 21, 30, 31]. Since *C. albicans* has become a prominent CAUTI pathogen, we explored its ability to grow in urine using clinical and laboratory strains. We used three urinary clinical isolates Pt62, Pt65, and PCNL1[27, 32] (obtained from Washington University School of Medicine) and two well-characterized laboratory strains, DAY230 and SC5314 (**Table S1**). Since hyphal formation is important for promoting disease, we used a hyphae defective mutant in the SC5314 background, *efg1*Δ*cph1*Δ, to test whether hyphal formation is important in the catheterized bladder environment (**Table S1**). We tested their ability to grow in a variety of environments ranging from nutrient rich to restrictive conditions. For rich environments, we used yeast extract peptone dextrose (YPD) and brain and heart infusion (BHI) in shaking and static conditions; YPD is a standard *C. albicans* growth media and BHI was used since the clinical strains were isolated on this media. Static growth was used to mimic the bladder environment and shaking growth was used as a comparison with standard lab culture conditions. For restrictive environments, we used human urine, and to further mimic the plasma protein extravasation in the catheterized bladder [28], urine was supplemented with either 3% human serum or different nitrogen sources including amino acids (AA), bovine serum albumin (BSA), or Fg. Serum albumin and Fg are two of the most abundant host proteins on catheters retrieved from humans and mice and have shown to be used by other uropathogens as a nutrient source [26, 33]. Samples were taken at 0 hours, 24 hours, and 48 hours to assess growth by enumeration of colony forming units (CFUs). As expected, *C. albicans* clinical and laboratory strains grow in higher densities in rich media and aeration while growth in rich media in static conditions was similar to the urine conditions (**Fig. S1**). In restrictive environments, *C. albicans* strains were able to survive and replicate in urine, but it varied widely between the strains and supplementation. Human serum supplementation promoted growth of all strains by 24 hrs with a subsequent decline except for Pt62, PCNL1, and DAY230, possibly because all nutrients were consumed rapidly (**Fig. 1A-F**). Supplementation with BSA or AA moderately promoted growth in all the strains except for DAY230 were it was inhibited when compared with urine alone (**Fig. 1A, D-F**). However, Fg enhanced growth of all strains, at different magnitudes when compared with urine alone (**Fig. 1A-F**).

Urine conditions promote *C. albicans* hyphal formation.

Environmental conditions induce *C. albicans* morphological changes that are associated with virulence [15, 18]. *C. albicans* can exhibit different morphologies [16], including yeast, pseudohyphae, and hyphae [15]. Hyphal morphology is associated with invasive growth and increased fungal virulence [17, 19]. Therefore, we determined how the bladder environment affects *C. albicans* morphology. To assess the pathogen morphologies, *C. albicans* laboratory and clinical strains were grown in urine with 10% human serum to mimic plasma protein extravasation in the catheterized bladder [28, 34]. YPD alone was used as a negative control and when supplemented with serum, was used as a positive control for inducing filamentation [35-37]. Strains were incubated at 37ºC with 5% CO_2 for 48 hrs and samples were collected at 0, 24, and 48 hours. *C. albicans* strains were stained with calcofluor white to assess morphology using fluorescence microscopy. Cell morphology analysis was done by quantifying the percentages of yeast, pseudohyphal, or hyphal forms (**Fig. 1M, Table S2**). All strains showed predominantly yeast morphology in YPD media, and YPD with serum induced pseudohyphal and hyphal formation in all strains, except Pt65 and SC5314 *efg1*Δ*cph1*Δ. Notably, our analysis showed that urine conditions promote pseudohyphal and hyphal formation in all strains (**Fig. 1G-K, Table S2**) except SC5314 *efg1*Δ*cph1*Δ (**Fig. 1L, Table S2**). Pseudohyphal and hyphal morphologies were further induced when urine was supplemented with human serum in all WT strains. This suggests that the catheterized environment triggers *C. albicans* morphological change from the yeast cell to hyphae.

Fibrinogen enhances *C. albicans* biofilm formation.

Scanning electron microscopy analyses of *C. albicans* biofilms on urinary catheters from CAUTI patients [13, 32] and rats [38, 39] have revealed pseudohyphal and hyphal morphologies. During candidiasis, *C. albicans* pseudohyphal and hyphal formation induces expression of virulence genes including host adhesion factors [14, 16, 40, 41] such as Mp58 (also named Pra1 in SC5314), a Fg-binding protein [42, 43]. In an *ex-vivo* study, we showed that *C. albicans* PCNL1 clinical isolate colocalized with Fg-deposited on urinary catheters retrieved from a patient with preoperative negative urine culture [27]. Fg deposition has been shown to be a platform for biofilm formation by diverse uropathogens [26, 27, 33, 44, 45], suggesting that Fg may be an important factor to promote *C. albicans* CAUTI pathogenesis. Based on these and our previous findings (**Fig. 1**), we hypothesized that urine conditions induce factors responsible for Fg-binding and biofilm formation. Thus, we assessed biofilm formation under rich (YPD and BHI) and restrictive conditions (human urine) and compared between BSA- and Fg-coated microplates as we have previously described [46]. At 48 hrs, immunostaining analyses were performed to assess fungal biofilm formation using anti-*Candida* antibodies, and biofilm biomass was quantified by fluorescence intensity [46]. We found that for the clinical strains, Fg promoted biofilm formation in all conditions, but Fg-dependent biofilm formation was further enhanced in human urine conditions (**Fig. 2A-C**). For the laboratory strains, we found a similar Fg-dependent biofilm formation in YPD, BHI, and urine, but Fg had no effect in DAY230 when grown in BHI (**Fig. 2D and E**). In contrast, SC5314 *efg1*Δ*cph1*Δ was not able to form biofilms in human urine regardless of the coated surface (**Fig. 2F**), highlighting the importance of filamentation for biofilms under urine conditions. Notably, we observed that all strains, including the hyphae-defective mutant, were able to form Fg-dependent biofilms in YPD and BHI (**Fig. 2A-F**), suggesting that the mechanisms of biofilm formation are different in restrictive and rich environments.

Fibrinogen promotes *C. albicans* biofilm formation.

We analyzed *C. albicans* biofilm formation by immunofluorescence (IF) microscopy. *C. albicans* biofilms were grown for 48 hrs in human urine using glass-bottom petri dishes coated with BSA or Fg. Biofilms on BSA were barely monolayers or small aggregates composed of yeast, pseudohyphae, and hyphae (**Fig. 2G-K**), except for SC5314 *efg1*Δ*cph1*Δ, where all cells were in yeast form (**Fig. 2L**). Fg promoted a robust biofilm in all strains when compared with BSA-dependent biofilms (**Fig. 2G-K**); except for the hyphae-deficient mutant where the colonization was composed of small yeast aggregates similar to the colonization on BSA-coated surfaces (**Fig. 2L**), suggesting filamentation is important for Fg-dependent biofilm formation.

Furthermore, in the damaged tissue environment, like the catheterized bladder, Fg is converted into fibrin fibers or meshes immediately to stop bleeding and allow tissue healing [47]. Therefore, we explored the fungal-fibrin interactions *in vitro*. Fibrin fibers and meshes were formed in glass-bottom petri dishes by adding thrombin to soluble Fg and incubating at 37°C; then, *C. albicans* strains were added and incubated for 48 hrs at 37°C in human urine. Visualization of the interaction was done by confocal microscopy and 3D reconstruction at 10x (**Fig. S2**) and 40x magnification (**Fig. 2M-R**). We found that most *C. albicans* cells had a pseudohyphal or hyphal morphology surrounding the fibrin fibers and meshes (**Fig. 2M-Q**), except for SC5314 *efg1*Δ*cph1*Δ strain (**Fig. 2R**), supporting that Fg-binding adhesins are expressed during hyphal morphogenesis.

C. albicans **hyphal formation is critical for establishment of CAUTI.**

Based on these results, we hypothesized that the *C. albicans* hyphae-deficient mutant would be deficient at colonization in the catheterized bladder. To test this, we assessed and compared the ability of the clinical and laboratory strains to colonize and form biofilms on the urinary catheter using our established CAUTI mouse model [26, 28, 33, 34, 44, 48-52]. To understand the contribution of the catheterized bladder environment to *C. albicans’* colonization, we compared fungal colonization in catheterized and non-catheterized mice. Mice with or without catheters were challenged with 1×10^6 CFU of each strain grown in YPD media overnight at 37°C under static conditions. After 24 hours post infection (hpi), the mice were euthanized and their organs and catheters (when catheterized) were harvested to quantify fungal colonization by CFU enumeration. Our results showed that catheterization significantly promotes bladder and catheter colonization by all the clinical and lab strains when compared to the bladder colonization in non-catheterized mice (**Fig. 3**). Importantly, bladder and catheter colonization by the hyphae-deficient mutant, SC5314 *efg1*Δ*cph1*Δ, were significantly impaired when compared with the SC5314 wild-type (WT) strain (p-value <0.005; **Fig. 3E**). Interestingly, in the absence of a catheter, the hyphae-deficient mutant behaved and colonized to the same extent as the WT strain.

In human infection, the incidence of candidemia and systemic dissemination arising from *Candida* UTI or candiduria (*Candida* in urine) are relatively low (1-8% of all candidemia cases)[53]. However, the prevalence of candidemia due to candiduria increases in critically ill and immunocompromised patients [54, 55], especially if the patients are undergoing urinary catheterization [56]. Since our mouse model of CAUTI allows us to assess dissemination, we analyzed fungal burden of kidneys, spleen, and heart after 24 hpi (**Fig. 3**). We found that urinary catheterization significantly contributes to the fungal spread of DAY230 to the kidneys and spleens (p-value <0.05; **Fig. 3D**) and in SC5314, spreads to the kidneys (p-value <0.005; **Fig. 3E**). Additionally, colonization of the kidneys by Pt62 and Pt65 was 2-3 logs higher than non-catheterized mice, trending to significance. Furthermore, the hyphae-deficient mutant, SC5314 *efg1*Δ*cph1*Δ, did not show differential dissemination between catheterized and non-catheterized mice (**Fig. 3E**). These data indicate that the changes induced by the presence of a catheter are necessary for fungal colonization of the urinary tract and further demonstrates that hyphal morphology, as well as pathways regulated by Efg1 and Cph1, are crucial for CAUTI establishment.

Fungal-fibrinogen interactions and hyphal morphology are important for *C. albicans* colonization of the catheterized bladder.

To further understand *C. albicans* morphogenesis, its interaction with Fg, and its spatial colonization in the bladder during CAUTI, we performed histological analyses using hematoxylin and eosin (H&E) staining, and IF microscopy of 24 hpi implanted and *C. albicans* infected bladders. For the IF analysis, we stained for *C. albicans* (red), Fg (green), and neutrophils (white) (**Fig. 4,** merge images; **Fig. S3-S8**, single channels). We focused on neutrophils for two reasons: we have shown they are highly recruited into the catheterized bladder [28, 34, 57], and neutropenic patients are more susceptible to *C. albicans* and bacterial dissemination from CAUTI [54, 58-60], suggesting a role in controlling candidemia from candiduria. We found that fungal bladder colonization was exceptionally robust and was visible in the H&E-stained whole bladders (blue arrow heads) (**Fig. 4**). Consistently, our IF analysis showed the presence of *C. albicans'* hyphal and pseudohyphal morphologies in the lumen of the bladder in all clinical and laboratory strains (**Fig 4A-E**), except for the hyphal-deficient mutant, SC5314 *efg1*Δ*cph1*Δ (**Fig. 4F**). Furthermore, *C. albicans* cells in the catheterized bladder are found associated with Fg (**Fig. 4** and **Fig. S3-S7**).

Neutrophils were highly recruited into the bladder, specifically in the areas with fungal colonization (**Fig. 4** and **Fig. S3-S7**). We found that *C. albicans* breached the urothelium, encountering a strong neutrophil response at the site of entry (**Fig. 4C-E** and **Fig. S5-S7**). For example, we found that PCNL1 was able to reach the bladder lamina propria, inducing a massive neutrophil recruitment to contain the infection (**Fig. 4C** and **Fig. S5**). Pt62 and Pt65 cells were primarily found on the bladder lumen and the fungal cells were interacting with Fg and neutrophils (**Fig. 4A-B** and **Fig. S3-S4**). On the other hand, robust fungal colonization and neutrophil recruitment was not observed in the SC5314 *efg1*Δ*cph1*Δ infected bladder (**Fig. 4F** and **Fig. S8**). These data demonstrate that in the catheterized bladder, *C. albicans* is mostly in hyphal and pseudohyphal morphologies, and it is able to interact with Fg. Furthermore, neutrophils are recruited to control fungal infection.

C. albicans interacts with deposited fibrinogen on the catheter during CAUTI.

Based on our *in vitro* Fg-binding results, we assessed if *C. albicans*-Fg interaction occurs *in vivo* on the catheter during CAUTI. Catheters from mice infected with each strain were retrieved 24 hpi and immunostained for *C. albicans* (red) and Fg (green). Except for the hyphal-deficient mutant, we found that all strains formed a robust biofilm on the implanted catheter (**Fig. 4G-R** merge images; **Fig. S9**, single channels), colonizing 59% to 79% of the surface of the catheter (**Table S3**). SC5314 WT showed 78.9 ± 14% colonization of the catheters while SC5314 *efg1*Δ*cph1*Δ catheters' colonization was 10.4 ± 7.5%, exhibiting a significant defective colonization (**Fig. 4L-M, R; Table S3**). Our IF analysis showed that *C. albicans* strains preferentially bound to deposited Fg on the catheter (**Fig. 4H-M and Fig. S9**). We then further quantified the percentage of the catheter-colonizing fungal population that was colocalizing with Fg. We found that 75% to 91% of the *C. albicans* strains staining was colocalized with deposited Fg (**Fig. 4N-R and Fig. S9**), even in the hyphal-deficient strain that was only able to colonize 10% of the catheter (**Fig. 4M, Table S3**), 79% of fungal was colocalizing with Fg (**Fig. 4R, Table S3**). This result further corroborates that hyphal formation is important for a robust biofilm formation during CAUTI and that Fg serves as a platform for catheter colonization *in vivo*.

Efg1 is critical for hyphal formation, Fg-dependent biofilm formation in urine, and development of CAUTI.

We next explored Efg1 and Cph1's independent contributions to hyphal morphology, Fg-dependent biofilm formation in urine conditions, and colonization of the catheterized bladder environment (**Fig. 5**). Using SN250 WT (SC5314 background), *cph1*Δ/Δ, and *efg1*Δ/Δ single mutants, we compared hyphal formation when grown in YPD and urine conditions in the presence or absence of human serum. We found that *cph1*Δ/Δ mutant was able to produce pseudohyphae and hyphae similarly to WT in urine supplemented with serum while the *efg1*Δ/Δ mutant remained mostly in the yeast form throughout all the conditions (**Fig. S10**), similar to the *efg1*Δ*cph1*Δ strain (**Fig. 1L**). We then tested the ability of these mutant strains to form Fg-dependent biofilm and interact with Fg fiber/meshes. We found that the *cph1*Δ/Δ mutant exhibits a ~40% decrease of biofilm formation when compared to the WT strains while *efg1*Δ/Δ mutant showed a ~95% reduction as the levels exhibit by *efg1*Δ*cph1*Δ strain (**Fig. 5A**). Furthermore, WT and *cph1*Δ/Δ showed a robust hyphal colonization surrounding the Fg fibers, differing from the *efg1*Δ/Δ mutant which showed few yeast cells bound directly to Fg mesh (**Fig. 5B and Fig. S2**) as also displayed by *efg1*Δ*cph1*Δ mutant (**Fig. 2R**). We further compared the ability of *cph1*Δ/Δ and *efg1*Δ/Δ to cause CAUTI. Mice were catheterized and challenged with $1x10^6$ CFU of the indicated strains and after 24 hpi, organs and catheters were harvested to quantify colonization by CFU enumeration. We found that *efg1*Δ/Δ was significantly defective in bladder (*p*-value < 0.002) and catheter colonization (*p*-value < 0.0002) while *cph1*Δ/Δ displayed comparable colonization to the WT strain (**Fig. 5C**). Furthermore, tissue bladder analysis showed that the *cph1*Δ/Δ infected bladder had an abundant hyphal burden similar to WT while the *efg1*Δ/Δ infected bladder showed defective colonization by yeast cells (**Fig. 5D; S11-S13**), similar to the *efg1*Δ*cph1*Δ strain (**Fig. 4F**). Moreover, robust neutrophil infiltration was observed in the bladder infected with WT and *cph1*Δ/Δ (**Fig. S11-S12**) but not in the *efg1*Δ/Δ infected bladder (**Fig. S13**). All these data show that Efg1 is the major transcriptional regulator responsible for activating pathways for survival and yeast-to-hyphal morphogenesis in the catheterized bladder environment, and is critical for establishment of CAUTI.

Als1 is important for biofilm formation in urine conditions and persistence during CAUTI.

We found that Fg acts as a fungal colonization platform in the catheterized bladder (**Fig. 4**), suggesting that urine conditions induce expression of Fg-binding adhesins. To identify key adhesins important for attachment, colonization, and persistence during CAUTI, we screened 12 adhesin mutants from the Shapiro library [61, 62] (**Fig. 6A**) and 27 adhesin mutants and biofilm-related from the Noble library [63] (**Fig. S14A**) for their ability to form Fg-dependent biofilms under urine conditions. We found that from all adhesin mutants, *als1*Δ/Δ exhibited a severe biofilm formation defect (**Fig. 6A**) similar to the ones produced by *efg1*Δ/Δ and *efg1*Δ*cph1*Δ (**Fig. 5A**). To confirm that the biofilm defect is due to the lack of the adhesin and not due to hyphal formation defect, we assessed hyphal morphology of the *als1*Δ/Δ mutant, finding no difference with the WT strain (**Fig. S15**). Based on the hypothesis that overexpression of Als1 could rescue the Fg-dependent biofilm defect, we compared biofilm formation between WT, *als1*Δ/Δ, and *ALS1* overexpression strains (OE; obtained from Shapiro lab, unpublished) on Fg-coated microplates under urine conditions for 48 hrs. We found that increased biomass was clearly visible in the *ALS1* OE strain (**Fig. S14B)**. The antibodies used for biofilm analysis were not able to accurately measure the *ALS1* OE biofilm due to its thickness. Therefore, we assessed the biofilm biomass via crystal violet staining, finding that the *ALS1* OE strain displayed an 8-fold increase in biomass compared to the WT strain (**Fig. 6B**). Additionally, we visualized the interaction of WT, *als1*Δ/Δ, and *ALS1* OE strains with fibrin, finding *als1*Δ/Δ strain showed less colonization of the fibrin meshes while *ALS1* OE exhibited a robust colonization similar to the WT strains (**Fig. 6C**).

We further compared the ability of WT, *als1*Δ/Δ, and *ALS1* OE strains to cause CAUTI. Catheterized mice were infected with 1x10^6 CFU of the indicated strains and 24 hpi organs and catheters were harvested to quantify colonization by CFU enumeration. We found that *als1*Δ/Δ displayed a significant defect in bladder (*p*-value <0.0006) and catheter colonization (*p*-value <0.0002) while *ALS1* OE showed a significant increase in bladder (*p*-value <0.002), catheter (*p*-value <0.03), and kidney (*p*-value <0.01) colonization when compared to WT strain (**Fig. 6D**). Furthermore, tissue bladder analysis of the *als1*Δ/Δ infected bladder did not show fungal colonization (**Fig. 6E**), whereas *ALS1* OE infected bladder had an abundant hyphal burden similar to WT (**Fig. 6E; Fig. S16-S18**). We then further quantified the percentage of the catheter-colonizing fungal population that colocalized with Fg. We found that catheter colonization by WT was on average 92.4%, *als1*Δ/Δ was ~10.73%, and *ALS1* OE was ~87.5. From that colonization, the fungal population colocalizing with deposited Fg was ~88.0% for WT, ~93.0 for *als1*Δ/Δ, and ~99.0% for *ALS1* OE (**Fig. 6F-G and Fig. S19**). Together these data show that Als1 is the Fg-binding protein critical for establishing colonization on the catheterized bladder and modulation of Als1 expression affects the outcome of infection.

DISCUSSION

Candida spp. CAUTIs are increasing, most commonly in prolonged urinary catheterization and ICU settings [64, 65]. Our results have shown that urinary catheterization significantly promotes colonization of the bladder by all the strains to $\geq 10^5$ CFU/ml whereas in the absence of the catheter, all the strains were unable to colonize and were present at $\leq 10^3$ CFU/ml (**Fig. 3**). According to the CDC criterion, a positive UTI is $\geq 10^5$ CFU/ml [66]. Our mouse model showed that urinary catheterization is required for fungal colonization, corroborating the clinical data.

In this study, we also found that Efg1-dependent hyphal morphology and Als1-mediated interactions with Fg and fibrin are critical for fungal CAUTI establishment (**Fig. 7**). We showed that *C. albicans* is able to survive and grow in urine and supplementation with 3% serum and Fg, conditions known to be present in the catheterized bladder, enhanced growth. Importantly, Efg1-dependent hyphal formation is promoted by urine *in vitro* and *C. albicans* strains exhibited pseudohyphal and hyphal morphologies *in vivo* during CAUTI. Importantly, *C. albicans* in hyphal formation induced a strong neutrophil recruitment to the bladder to control the fungal infection. The presence of Fg and fibrin enhanced Als1-dependent biofilm formation *in vitro* and *in vivo*. Thus, the catheterized bladder creates the ideal environment for *C. albicans* to colonize and persist in the host.

In clinical settings, there is frequently a dilemma in distinguishing fungal colonization from an infection and whether to treat candiduria or not [1-3]. Therefore, it is important to differentiate if *C. albicans* behaves as a commensal or pathogen during colonization in the catheterized bladder. Noble and Pavelka's groups suggest that yeast morphology leads to commensalism while filamentation promotes infection and invasive colonization [67, 68]. Their reports have shown a balance between commensalism (yeast form) and invasive phenotypes (hyphal morphology) in the gut that antagonize each other [67, 68]. Specifically, spontaneous mutations in Efg1 and other hyphal genes allow *C. albicans* to adapt to commensalism in the gut [67]. Furthermore, the Tang group showed that under normal conditions in the GI tract – the *C. albicans* reservoir – this yeast behaves as a commensal [69]. However, when the intestinal mucosa is damaged, *C. albicans* switches from yeast to hyphal morphology to take advantage of the impaired intestinal mucosal barrier [69]. We know that urinary catheterization causes mechanical damage to the bladder, inducing epithelial wounding and triggering a robust inflammation [28, 70], and several clinical studies have detected *C. albicans* hyphae and biofilms on indwelling urinary catheters retrieved from patients with candiduria [13, 71, 72], suggesting fungal pathogenic programming during CAUTI. Here, we demonstrated that urine induces hyphal morphology *in vitro* and *in vivo* (**Fig. 1 and Table S2**), and the Efg1-dependent hyphal programming is critical for bladder and catheter colonization (**Fig. 5**). Furthermore, a strong neutrophil recruitment during hyphal colonization (WT and *cph1*Δ/Δ strains) of the catheterized bladder was observed (**Fig. 5**). This observation is important since commensal *C. albicans* promote immune tolerance as "peaceful coexistence" [73], while the host will evoke an active immune and inflammatory responses to invasive fungi [74]. Based on previous studies and our results, this suggests that *C. albicans* has a pathogenic programming in response to the catheterized bladder environment, resulting in fungal CAUTI.

During CAUTI, neutrophils are robustly recruited to the bladder as a defense mechanism against invading pathogens and their numbers increase with extended catheterization [28, 57]. In neutropenic mice, the bacterial burden increases 10-fold during CAUTI, suggesting that neutrophils are controlling and containing the infection in the bladder [28]. Similarly, neutropenic patients developed candidemia from candiduria, suggesting that bladder recruited neutrophils are critical to control fungal systemic dissemination [54]. Neutrophils have shown to be the major immune cells in the control of candidiasis [75] by phagocytizing and killing yeast cells and short hyphae, while large hyphae are killed by inducing neutrophil extracellular traps (NETs), which releases DNA, granule enzymes, and antimicrobial peptides [76]. Our future studies will be focused on understanding the immune cell strategies against the fungal CAUTI and their role in containing the fungal infection in the bladder.

Host proteins have been shown to contribute to fungal biofilm formation [39]. We demonstrated that Fg is accumulated in the bladder and deposited on the catheters [9, 27] and that *C. albicans* PCNL1 clinical isolate colocalized with Fg-deposited on urinary catheters retrieved from a patient with preoperative negative urine culture [27]. Moreover, a study from the Andes group showed that Fg, as well as other host proteins, were associated with *C. albicans* biofilms in urinary catheters retrieved from rats [20]. Therefore, we focused on understanding Fg's role in *C. albicans* CAUTI. We found that hyphal formation was critical for Fg-dependent biofilm formation in urine conditions but not in YPD and BHI media, while the hyphal-defective mutant was not able to form Fg-dependent biofilms in urine, but could in YPD and BHI (**Fig. 1**). This seemingly contradictory result is not surprising since we have observed that laboratory growth media does not fully recapitulate conditions found within the host. For example, several factors critical for bacterial biofilm formation in CAUTI are dispensable in *in vitro* biofilm assays when using conventional laboratory growth media [26, 34]. This difference could be related to adhesins that are expressed in yeast that may contribute to biofilm growth in laboratory conditions. Therefore, using conditions that closely mimic the *in vivo* environment are important to identify physiologically-relevant determinants for CAUTI colonization and survival.

Furthermore, we found that Fg enhances fungal biofilm formation in urine conditions and during urinary catheterization and is mediated by the adhesin, Als1 (**Fig. 3, 5-6**). We found that modulation of Als1 affected the outcome of biofilm formation and infection, finding that *C. albicans als1Δ/Δ* strain displayed defective Fg-dependent biofilm formation *in vitro* and *in vivo* colonization while *ALS1* overexpression strain rescues Fg-dependent biofilm and *C. albicans* CAUTI (**Fig. 6**). Previous structural studies showed that the N-terminal domain of Als1 interacts with Fg [77, 78], binding to the Fg γ-chain via protein-protein interaction, similar to Clf adhesins in *S. aureus* [78, 79]. Als1 belongs to the agglutinin-like sequences (Als) protein family of cell-surface glycoproteins, which are important for adhesion to host, bacteria, and abiotic surfaces [77]. Interestingly, Als3 and Als9-2 (an allelic variant of *ALS9*) has been shown to interact with Fg [77, 78]; however, they are dispensable in the Fg-dependent biofilm in urine conditions (**Fig. 6a**). This may suggest that these factors are not expressed under urine conditions. It is known that Als1 is a Efg1-downstream target [80]. However, some studies have also shown that Efg1 regulates Als3 expression under serum conditions [80] but Efg1 direct binding to Als3 promoter has not been proven, suggesting that Efg1 binds to the promoter regions under specific environmental cues or Efg1 may regulate *ALS3* indirectly via other target proteins [80]. Efg1 has both overlapping and distinct targets under different environmental conditions [80]. Therefore, future studies dissecting the Efg1 regulatory network in the catheterized bladder will be crucial to understand *C. albicans* cellular signaling and to better manage the outcome of infection.

C. albicans occupies many niches in the human body, and morphological changes are associated with the establishment of diseased states. This is important in the bladder, since it is an open and dynamic system, where urine is constantly passing through. Therefore, in order to establish a successful colonization, adhesion and biofilm formation on the urinary catheter is essential [26, 52]. Our results are consistent with that; *Candida* biofilms not only ensures colonization but can protect the growing cells from the hostile environment and potentiate establishment of the infection [81]. This is the first study unveiling *C. albicans* mechanism of pathogenesis during CAUTI, finding that Efg1, and specifically its downstream target Als1, are critical for establishing infection. This study opens new avenues to understanding *C. albicans* cellular programming in the catheterized bladder. Importantly, the key interaction of Als1-Fg, an initial step for colonization, could be exploited as a potential therapeutic avenue to prevent *C. albicans* CAUTIs.

MATERIALS AND METHODS

Ethics statement. All animal care was consistent with the Guide for the Care and Use of Laboratory Animals from the National Research Council. The University of Notre Dame Institutional Animal Care and Use Committee approved all mouse infections and procedures as part of protocol number 18-08-4792MD. For urine and blood collections, all donors signed an informed consent form and protocols were approved by the Institutional Review Board of the University of Notre Dame under study #19-04-5273 for urine and #18-08-4834 for blood.

Urine Collection. Human urine from at least two healthy female donors between the ages of 20 - 35 were collected and pooled. Donors did not have a history of kidney disease, diabetes, or recent antibiotic treatment. Urine was sterilized with a 0.22 µm filter (VWR 29186-212) and pH was normalized to 6.0-6.5. BSA (VWR 97061-48) supplemented urine was sterilized again using a 0.22 µm filter. When urine was supplemented with Fg (Enzyme Research Laboratories FIB 3), it was added directly to the sterilized urine and the urine was not sterilized after the addition of Fg.

Fungal Culture Conditions. All strains of *Candida albicans* were cultured at 37 °C with aeration in 5 mL of YPD (10g/L Yeast Extract (VWR J850-500G), 20g/L Peptone (VWR J636-500G), 20 g/L Dextrose (VWR BDH9230-500G)) broth. For *in vivo* mouse experiments, *C. albicans* strains were grown static overnight in 10 mL of YPD.

Growth Curve. Growth curves were performed in glass test tubes (Thermo Fisher Scientific 14-961-29). Overnight cultures (all in stationary phase; measured using a UV/Vis Spectrophotometer) were normalized to ~1x10^6 CFU/ml in 1xPBS (Sigma–Aldrich 1002786391). The culture was then diluted (1:1000) into human urine (supplemented with 1 mg/mL BSA, 1 mg/mL Fg, 50X amino acids, or 1 mg/mL human serum), BHI (incubated statically or shaking), or YPD (incubated statically or shaking) and were incubated in the test tube at 37ºC for 48 hours. At 0, 24, and 48 hours, samples of each condition were taken and analyzed by CFU counts.

Morphology Assay and Analysis. All strains of *C. albicans* were grown in YPD with or without serum and in human urine with or without serum. At 0, 24, and 48 hours, a sample of each condition was taken, fixed with 10% formalin, and stained with 100 µg/mL of calcofluor. Samples were viewed under a Zeiss inverted light microscope (Carl Zeiss, Thornwood, NY) with the DAPI fluorescent channel. Random images were taken at 100x magnification and processed with manual counting of yeast, pseudohyphae, and hyphae phenotypes. Images (consisting of a 3 x 3 tiled region, i.e. 9 fields of view) were randomly acquired and at least three images were analyzed per condition. The total number of cells per phenotype were summed and divided by the total number of cells to give the overall percentage of each cell type on Microsoft Excel.

Antibodies and dyes used in this study.

Primary antibodies: Goat anti-fibrinogen (Sigma-Aldrich F8512), rabbit anti-*Candida* (ThermoFisher Scientific PA1-27158), and rat anti-mouse Ly6G (BD Pharmingen 551459). **Secondary antibodies**: Alexaflour 488-labeled donkey anti-goat (ThermoFisher Scientific SA5-

10086); Alexaflour 594-labeled donkey anti-rabbit (ThermoFisher Scientific SA5-10039); Alexaflour 647-labeled donkey anti-rat (ThermoFisher Scientific SA5-10029); IRDye 800CW donkey anti-goat; and IRDye 680LT donkey anti-rabbit. Alexaflour secondary antibodies were purchased from Invitrogen Molecular Probes and IRDye conjugates secondary antibodies from LI-COR Biosciences. **Dyes:** Calcofluor white (Fluorescent Brightener 28, Sigma F3543) staining; Hoechst dye (Thermo Fisher Scientific 62249) staining; Hematoxylin and Eosin (H&E) (vector Laboratories #H-3502).

Biofilm Formation in 96-well plates. Biofilm formations were performed in 96 well flat-bottomed plates (VWR 10861-562) coated with 100uL of BSA or Fg (150 µg/mL) incubated overnight at 4°C. The various strains were grown as described above and the inoculum normalized to ~1x10^6 CFU/ml. Cultures were then diluted (1:1000) into YPD, BHI, or human urine. 100uL of the inoculum were incubated in the wells of the 96 well plate at 37ºC for 48 hours while static.

Following the 48hr incubation, the supernatant was removed from the plate and washed three times with 200uL 1x PBS to remove unbound fungi. Plates were fixed with 10% neutralizing formalin (Leica 3800600) for 20 minutes and followed by three washes with PBS containing 0.05% Tween-20 (PBS-T). Blocking solution (PBS with 1.5% BSA and 0.1% sodium azide (Acros Organics 447811000)) was added to the plate for one hour at room temperature and then washed with PBS-T (3x). Biofilms were incubated with anti-*Candida* antibodies diluted into dilution buffer (PBS with 0.05% Tween (VWR M147-1L), 0.1% BSA) for two hours. Plates were washed three times with PBS-T and incubated for one hour with IRDye 680 LT donkey anti-rabbit secondary antibody solution at room temperature and washed with PBS-T (3x). As a final step, the biofilms were visualized by scanning the plates using the Odyssey Imaging System (LI-COR Biosciences) and the analyzed with Image Studio software to obtain the fluorescence intensities (LI-COR Version 5.2, Lincoln, NE).

BSA or Fg-coated dishes and formation of Fibrin fibers/nets. For these assays No. 0 coverglass glass-bottom 35 mm petri dish with a 14 mm microwell (MatTek P35G-0-14-C) were used. The dishes were coated with 150 µg/mL of BSA or Fg overnight at 4°C. For fibrin fiber/nets formation, Fg and thrombin (Sigma-Aldrich T6884-250UN) were thawed at 37°C. 100 µl of 0.5 mg/ml Fg in PBS was added into the microwell glass-bottom and then 10 µl of 2 U/ml thrombin was added to polymerize Fg into fibrin. Dishes were incubated at 37°C for 1 hour and kept overnight at 4°C

Visualization of biofilms and fungal-fibrin interaction. The various strains were grown as described above and the inoculum normalized to ~1x10^6 CFU/ml in PBS. These cultures were then diluted (1:1000) into human urine, added to the BSA-, Fg-, or fibrin coated dishes and then were incubated at 37ºC for 48 hours under static conditions. After incubation, dishes were then washed three times with 1x PBS to remove unbound fungi, then dishes were fixed with 10% neutralizing formalin solution for 20 minutes and washed with 1x PBS three times. Dishes were blocked with blocking solution for an hour at room temperature as described above. Then BSA- and Fg-coated dishes were incubated in primary antibody (rabbit anti-*Candida*) and for fibrin-coated dishes were incubated with rabbit anti-*Candida* and goat anti-Fg antibodies. Incubation with the primary antibodies was done for two hours followed by three washes with PBS-T. Then, dishes were incubated for 1 hour with Alexaflour 594-labeled donkey anti-rabbit secondary antibody for BSA- and Fg-coated dishes and Alexaflour 594-labeled donkey anti-rabbit and Alexaflour 488-labeled donkey anti-goat antibodies for fibrin-coated dishes, followed by three washes with PBS-T. BSA- and Fg- coated dishes were visualized with a Zeiss inverted light microscope, and images were taken at different magnifications (10x, 20x, 40x and 100x). Zen Pro and Fiji-ImageJ [82] softwares were used to analyze the images. For the fungal-fibrin interaction, fibrin-coated dishes were visualized by Nikon A1-R/Multi-Photon Laser Scanning Confocal Microscope and images were analyzed by IMARIS Image Analysis software and ImageJ software [82].

Crystal Violet Staining. Following biofilm formation on Fg-coated microplate, the supernatant was removed, and the plate was incubated in 200 µl of 0.5% crystal violet for 15 minutes. Crystal violet stain was removed, and the plate was washed with water to remove remaining stain. Plates were dried and then incubated with 200 µl of 33% acetic acid for 15 minutes. In a new plate, 100 µl of the acetic acid solution was transferred, and absorbance values were measured via a plate spectrophotometer at 595 nm.

***In Vivo* Mouse Model.** Mice used in this study were ~6-week-old female wild-type C57BL/6 mice purchased from Jackson Laboratory. Mice were subjected to transurethral implantation of a silicone catheter and inoculated as previously described[50]. Briefly, mice were anesthetized by inhalation of isoflurane and implanted with a 6-mm-long silicone catheter (BrainTree Scientific SIL 025). Mice were infected immediately following catheter implantation with 50□µl of ∼1□×□10^6 CFU/mL in PBS, of one of the fungal strains introduced into the bladder lumen by transurethral inoculation. Mice were sacrificed at 24 hours post infection by cervical dislocation after anesthesia inhalation and catheter, bladder, kidneys, spleen, and heart were aseptically harvested. Organs were homogenized and catheters were cut in small pieces before sonication for fungal CFU enumeration. A subset of catheters were fixed for imaging as described below and a subset of bladders were fixed and processed for immunofluorescence and histology analysis as described below.

Catheter Imaging and Analysis. Harvested catheters were fixed for imaging via standard IF procedure as previously described [49]. Briefly, catheters were fixed with formalin, blocked, washed with 1x PBS, and incubated with the appropriate primary antibodies overnight. Catheters were then incubated with secondary antibodies for 2 hrs at room temperature. Catheters were washed with PBS-T and then a final wash with PBS. Catheters were visualized with the Odyssey Imaging System and then analyzed using color pixel counter from Fiji-ImageJ software [82]. The number of pixels of each color was compared to the total number of pixels to identify percent coverage of the catheter.

Bladder IHC and H&E Staining of Mouse Bladders. Mouse bladders were fixed in 10% formalin overnight, before being processed for sectioning and staining as previously described [52]. Briefly, bladder sections were deparaffinized, rehydrated, and rinsed with water. Antigen retrieval was accomplished by boiling the samples in Na-citrate, washing in tap water, and then incubating in 1x PBS three times. Sections were then blocked (1% BSA, 0.3% TritonX100 (Acros Organics 21568-2500) in 1x PBS) washed in 1x PBS, and incubated with appropriate primary antibodies diluted in blocking buffer overnight at 4 °C. Next, sections were washed with 1x PBS, incubated with secondary antibodies for 2 hrs at room temperature, and washed once more in 1x PBS prior to Hoechst dye staining. Secondary antibodies for immunohistochemistry were Alexa 488 donkey anti-goat, Alexa 550 donkey anti-rabbit, and Alexa 650 donkey anti-rat. Hematoxylin and Eosin (H&E) stain for light microscopy was done by the CORE facilities at the University of Notre Dame (ND CORE). All imaging was done using a Zeiss inverted light microscope and a Nikon A1-R/Multi-Photon Laser Scanning Confocal Microscope. Zen Pro,ImageJ software, and IMARIS Image Analysis software were used to analyze the images.

Statistical Analysis. Data from at least 3 experiments were pooled for each assay. Two-tailed Mann-Whitney *U* tests were performed with GraphPad Prism 5 software (GraphPad Software, San Diego, CA) for all comparisons described in biofilm, CAUTI, and catheter coverage experiments. Values represent means ± SEM derived from at least 3 independent experiments. *, $P<0.05$; **, $P<0.005$; ***, $P<0.0005$; ns, difference not significant.

REFERENCES

1. Alfouzan WA, Dhar R. Candiduria: Evidence-based approach to management, are we there yet? J Mycol Med. 2017;27(3):293-302. Epub 2017/05/16. doi: 10.1016/j.mycmed.2017.04.005. PubMed PMID: 28501465.
2. Fisher JF. Candiduria: When and How to Treat It. Curr Infect Dis Rep. 2000;2(6):523-30. Epub 2000/11/30. doi: 10.1007/s11908-000-0056-2. PubMed PMID: 11095903.
3. Hollenbach E. To treat or not to treat--critically ill patients with candiduria. Mycoses. 2008;51 Suppl 2:12-24. Epub 2008/09/09. doi: 10.1111/j.1439-0507.2008.01570.x. PubMed PMID: 18721329.
4. Antibiotic resistance threats in the United States, 2019. 2019. PubMed PMID: cdc:82532.
5. Geddes-McAlister J, Shapiro RS. New pathogens, new tricks: emerging, drug-resistant fungal pathogens and future prospects for antifungal therapeutics. Ann N Y Acad Sci. 2019;1435(1):57-78. Epub 2018/05/16. doi: 10.1111/nyas.13739. PubMed PMID: 29762860.
6. Sanguinetti M, Posteraro B, Lass-Flörl C. Antifungal drug resistance among Candida species: mechanisms and clinical impact. Mycoses. 2015;58 Suppl 2:2-13. Epub 2015/06/03. doi: 10.1111/myc.12330. PubMed PMID: 26033251.
7. Sobel JD, Fisher JF, Kauffman CA, Newman CA. Candida urinary tract infections--epidemiology. Clin Infect Dis. 2011;52 Suppl 6:S433-6. Epub 2011/04/22. doi: 10.1093/cid/cir109. PubMed PMID: 21498836.
8. Fisher JF, Sobel JD, Kauffman CA, Newman CA. Candida urinary tract infections--treatment. Clin Infect Dis. 2011;52 Suppl 6:S457-66. Epub 2011/04/22. doi: 10.1093/cid/cir112. PubMed PMID: 21498839.

9. Flores-Mireles A, Hreha TN, Hunstad DA. Pathophysiology, Treatment, and Prevention of Catheter-Associated Urinary Tract Infection. Top Spinal Cord Inj Rehabil. 2019;25(3):228-40. Epub 2019/09/25. doi: 10.1310/sci2503-228. PubMed PMID: 31548790; PubMed Central PMCID: PMCPMC6743745.

10. Maki DG, Tambyah PA. Engineering out the risk for infection with urinary catheters. Emerg Infect Dis. 2001;7(2):342-7. doi: 10.3201/eid0702.010240. PubMed PMID: 11294737.

11. Rogers MA, Mody L, Kaufman SR, Fries BE, McMahon LF, Jr., Saint S. Use of urinary collection devices in skilled nursing facilities in five states. J Am Geriatr Soc. 2008;56(5):854-61. Epub 2008/05/06. doi: 10.1111/j.1532-5415.2008.01675.x. PubMed PMID: 18454750.

12. Montoya A, Mody L. Common infections in nursing homes: a review of current issues and challenges. Aging health. 2011;7(6):889-99. Epub 2012/12/25. doi: 10.2217/ahe.11.80. PubMed PMID: 23264804; PubMed Central PMCID: PMCPMC3526889.

13. Fisher JF, Kavanagh K, Sobel JD, Kauffman CA, Newman CA. Candida urinary tract infection: pathogenesis. Clin Infect Dis. 2011;52 Suppl 6:S437-51. Epub 2011/04/22. doi: 10.1093/cid/cir110. PubMed PMID: 21498837.

14. Mayer FL, Wilson D, Hube B. Candida albicans pathogenicity mechanisms. Virulence. 2013;4(2):119-28. Epub 2013/01/11. doi: 10.4161/viru.22913. PubMed PMID: 23302789; PubMed Central PMCID: PMCPMC3654610.

15. Thompson DS, Carlisle PL, Kadosh D. Coevolution of morphology and virulence in Candida species. Eukaryot Cell. 2011;10(9):1173-82. Epub 2011/07/19. doi: 10.1128/EC.05085-11. PubMed PMID: 21764907; PubMed Central PMCID: PMCPMC3187052.

16. Noble SM, Gianetti BA, Witchley JN. Candida albicans cell-type switching and functional plasticity in the mammalian host. Nat Rev Microbiol. 2017;15(2):96-108. Epub 2016/11/22. doi: 10.1038/nrmicro.2016.157. PubMed PMID: 27867199; PubMed Central PMCID: PMCPMC5957277.

17. Sudbery PE. Growth of Candida albicans hyphae. Nat Rev Microbiol. 2011;9(10):737-48. Epub 2011/08/17. doi: 10.1038/nrmicro2636. PubMed PMID: 21844880.

18. Nobile CJ, Johnson AD. Candida albicans Biofilms and Human Disease. Annu Rev Microbiol. 2015;69:71-92. Epub 2015/10/22. doi: 10.1146/annurev-micro-091014-104330. PubMed PMID: 26488273; PubMed Central PMCID: PMCPMC4930275.

19. Pukkila-Worley R, Peleg AY, Tampakakis E, Mylonakis E. Candida albicans Hyphal Formation and Virulence Assessed Using a Caenorhabditis elegans Infection Model. Eukaryotic Cell. 2009;8(11):1750-8. doi: 10.1128/Ec.00163-09. PubMed PMID: WOS:000271368700013.

20. Nett JE, Andes DR. Contributions of the Biofilm Matrix to Candida Pathogenesis. J Fungi (Basel). 2020;6(1). Epub 2020/02/08. doi: 10.3390/jof6010021. PubMed PMID: 32028622; PubMed Central PMCID: PMCPMC7151000.

21. Tsui C, Kong EF, Jabra-Rizk MA. Pathogenesis of Candida albicans biofilm. Pathog Dis. 2016;74(4):ftw018. Epub 2016/03/11. doi: 10.1093/femspd/ftw018. PubMed PMID: 26960943; PubMed Central PMCID: PMCPMC5975230.

22. Pristov KE, Ghannoum MA. Resistance of Candida to azoles and echinocandins worldwide. Clinical Microbiology and Infection. 2019;25(7):792-8. doi: https://doi.org/10.1016/j.cmi.2019.03.028.

23. Garibaldi RA, Burke JP, Dickman ML, Smith CB. Factors predisposing to bacteriuria during indwelling urethral catheterization. The New England journal of medicine. 1974;291(5):215-9. doi: 10.1056/NEJM197408012910501. PubMed PMID: 4834750.

24. Norden CW, Green GM, Kass EH. Antibacterial mechanisms of the urinary bladder. The Journal of clinical investigation. 1968;47(12):2689-700. Epub 1968/12/01. doi: 10.1172/JCI105952. PubMed PMID: 4881768; PubMed Central PMCID: PMC297440.

25. Warren JW. Catheter-associated urinary tract infections. Infectious disease clinics of North America. 1997;11(3):609-22. Epub 1997/10/06. PubMed PMID: 9378926.

26. Flores-Mireles AL, Pinkner JS, Caparon MG, Hultgren SJ. EbpA vaccine antibodies block binding of Enterococcus faecalis to fibrinogen to prevent catheter-associated bladder infection in mice. Sci Transl Med. 2014;6(254):254ra127. Epub 2014/09/19. doi: 10.1126/scitranslmed.3009384. PubMed PMID: 25232179; PubMed Central PMCID: PMCPMC4365981.

27. Flores-Mireles AL, Walker JN, Bauman TM, Potretzke AM, Schreiber HLt, Park AM, et al. Fibrinogen Release and Deposition on Urinary Catheters Placed during Urological Procedures. J Urol. 2016;196(2):416-21. Epub 2016/02/02. doi: 10.1016/j.juro.2016.01.100. PubMed PMID: 26827873; PubMed Central PMCID: PMCPMC4965327.

28. Guiton PS, Hannan TJ, Ford B, Caparon MG, Hultgren SJ. Enterococcus faecalis overcomes foreign body-mediated inflammation to establish urinary tract infections. Infect Immun. 2013;81(1):329-39. Epub 2012/11/08. doi: 10.1128/IAI.00856-12. PubMed PMID: 23132492; PubMed Central PMCID: PMCPMC3536162.

29. Andersen MJ, Fong C, La Bella AA, Molina JJ, Molesan A, Champion MM, et al. Inhibiting host-protein deposition on urinary catheters reduces associated urinary tract infections. Elife. 2022;11. Epub 2022/03/30. doi: 10.7554/eLife.75798. PubMed PMID: 35348114; PubMed Central PMCID: PMCPMC8986317.

30. Alves R, Barata-Antunes C, Casal M, Brown AJP, Van Dijck P, Paiva S. Adapting to survive: How Candida overcomes host-imposed constraints during human colonization. Plos Pathog. 2020;16(5). doi: ARTN e100847810.1371/journal.ppat.1008478. PubMed PMID: WOS:000538054300041.

31. Flores-Mireles AL, Walker JN, Caparon M, Hultgren SJ. Urinary tract infections: epidemiology, mechanisms of infection and treatment options. Nat Rev Microbiol. 2015;13(5):269-84. Epub 2015/04/09. doi: 10.1038/nrmicro3432. PubMed PMID: 25853778; PubMed Central PMCID: PMCPMC4457377.

32. Walker JN, Flores-Mireles AL, Lynch AJL, Pinkner C, Caparon MG, Hultgren SJ, et al. High-resolution imaging reveals microbial biofilms on patient urinary catheters despite antibiotic administration. World J Urol. 2020;38(9):2237-45. Epub 2019/12/04. doi: 10.1007/s00345-019-03027-8. PubMed PMID: 31792577.

33. Flores-Mireles AL, Walker JN, Potretzke A, Schreiber HL, Pinkner JS, Bauman TM, et al. Antibody-Based Therapy for Enterococcal Catheter-Associated Urinary Tract Infections. Mbio. 2016;7(5). doi: ARTN e01653-1610.1128/mBio.01653-16. PubMed PMID: WOS:000390132900017.

34. Guiton PS, Hung CS, Hancock LE, Caparon MG, Hultgren SJ. Enterococcal biofilm formation and virulence in an optimized murine model of foreign body-associated urinary tract infections. Infect Immun. 2010;78(10):4166-75. Epub 2010/08/11. doi: 10.1128/IAI.00711-10. PubMed PMID: 20696830; PubMed Central PMCID: PMC2950371.

35. Bar-Yosef H, Vivanco Gonzalez N, Ben-Aroya S, Kron SJ, Kornitzer D. Chemical inhibitors of Candida albicans hyphal morphogenesis target endocytosis. Sci Rep. 2017;7(1):5692. Epub 2017/07/20. doi: 10.1038/s41598-017-05741-y. PubMed PMID: 28720834; PubMed Central PMCID: PMCPMC5515890.

36. Watanabe H, Azuma M, Igarashi K, Ooshima H. Relationship between cell morphology and intracellular potassium concentration in Candida albicans. J Antibiot. 2006;59(5):281-7. doi: DOI 10.1038/ja.2006.39. PubMed PMID: WOS:000238172500002.

37. Feng QH, Summers E, Guo B, Fink G. Ras signaling is required for serum-induced hyphal differentiation in Candida albicans. J Bacteriol. 1999;181(20):6339-46. doi: Doi 10.1128/Jb.181.20.6339-6346.1999. PubMed PMID: WOS:000083006500016.

38. Nett JE, Brooks EG, Cabezas-Olcoz J, Sanchez H, Zarnowski R, Marchillo K, et al. Rat indwelling urinary catheter model of Candida albicans biofilm infection. Infect Immun. 2014;82(12):4931-40. Epub 2014/09/04. doi: 10.1128/IAI.02284-14. PubMed PMID: 25183731; PubMed Central PMCID: PMCPMC4249295.

39. Nett JE, Zarnowski R, Cabezas-Olcoz J, Brooks EG, Bernhardt J, Marchillo K, et al. Host contributions to construction of three device-associated Candida albicans biofilms. Infect Immun. 2015;83(12):4630-8. Epub 2015/09/16. doi: 10.1128/IAI.00931-15. PubMed PMID: 26371129; PubMed Central PMCID: PMCPMC4645408.

40. Schaller M, Borelli C, Korting HC, Hube B. Hydrolytic enzymes as virulence factors of Candida albicans. Mycoses. 2005;48(6):365-77. Epub 2005/11/03. doi: 10.1111/j.1439-0507.2005.01165.x. PubMed PMID: 16262871.

41. Carlisle PL, Banerjee M, Lazzell A, Monteagudo C, Lopez-Ribot JL, Kadosh D. Expression levels of a filament-specific transcriptional regulator are sufficient to determine Candida albicans morphology and virulence. P Natl Acad Sci USA. 2009;106(2):599-604. doi: 10.1073/pnas.0804061106. PubMed PMID: WOS:000262804000045.

42. Casanova M, Lopez-Ribot JL, Monteagudo C, Llombart-Bosch A, Sentandreu R, Martinez JP. Identification of a 58-kilodalton cell surface fibrinogen-binding mannoprotein from *Candida albicans*. Infect Immun. 1992;60(10):4221-9. PubMed PMID: 1398933; PubMed Central PMCID: PMC257456.

43. Sepulveda P, Lopez-Ribot JL, Murgui A, Canton E, Navarro D, Martinez JP. *Candida albicans* fibrinogen binding mannoprotein: expression in clinical strains and immunogenicity in patients with candidiasis. International microbiology : the official journal of the Spanish Society for Microbiology. 1998;1(3):209-16. PubMed PMID: 10943362.

44. Gaston JR, Andersen MJ, Johnson AO, Bair KL, Sullivan CM, Guterman LB, et al. Enterococcus faecalis Polymicrobial Interactions Facilitate Biofilm Formation, Antibiotic Recalcitrance, and Persistent Colonization of the Catheterized Urinary Tract. Pathogens. 2020;9(10). doi: ARTN 83510.3390/pathogens9100835. PubMed PMID: WOS:000586941800001.

45. Walker JN, Flores-Mireles AL, Pinkner CL, Schreiber HL, Joens MS, Park AM, et al. Catheterization alters bladder ecology to potentiate Staphylococcus aureus infection of the urinary tract. P Natl Acad Sci USA. 2017;114(41):E8721-E30. doi: 10.1073/pnas.1707572114. PubMed PMID: WOS:000412653900023.

46. Colomer-Winter C, Lemos JA, Flores-Mireles AL. Biofilm Assays on Fibrinogen-coated Silicone Catheters and 96-well Polystyrene Plates. Bio Protoc. 2019;9(6). Epub 2019/05/21. doi: 10.21769/BioProtoc.3196. PubMed PMID: 31106237; PubMed Central PMCID: PMCPMC6519467.

47. Weisel JW, Litvinov RI. Fibrin Formation, Structure and Properties. Subcell Biochem. 2017;82:405-56. Epub 2017/01/20. doi: 10.1007/978-3-319-49674-0_13. PubMed PMID: 28101869; PubMed Central PMCID: PMCPMC5536120.

48. Colomer-Winter C, Flores-Mireles AL, Baker SP, Frank KL, Lynch AJL, Hultgren SJ, et al. Manganese acquisition is essential for virulence of Enterococcus faecalis. Plos Pathog. 2018;14(9):e1007102. Epub 2018/09/21. doi: 10.1371/journal.ppat.1007102. PubMed PMID: 30235334; PubMed Central PMCID: PMCPMC6147510.

49. Colomer-Winter C, Flores-Mireles AL, Kundra S, Hultgren SJ, Lemos JA. (p)ppGpp and CodY Promote Enterococcus faecalis Virulence in a Murine Model of Catheter-Associated Urinary Tract Infection. mSphere. 2019;4(4). Epub 2019/07/26. doi: 10.1128/mSphere.00392-19. PubMed PMID: 31341072; PubMed Central PMCID: PMCPMC6656871.

50. Conover MS, Flores-Mireles AL, Hibbing ME, Dodson K, Hultgren SJ. Establishment and Characterization of UTI and CAUTI in a Mouse Model. J Vis Exp. 2015;(100):e52892. Epub 2015/07/02. doi: 10.3791/52892. PubMed PMID: 26132341; PubMed Central PMCID: PMCPMC4544389.

51. Di Venanzio G, Flores-Mireles AL, Calix JJ, Haurat MF, Scott NE, Palmer LD, et al. Urinary tract colonization is enhanced by a plasmid that regulates uropathogenic Acinetobacter baumannii chromosomal genes. Nat Commun. 2019;10. doi: ARTN 276310.1038/s41467-019-10706-y. PubMed PMID: WOS:000472598000004.

52. Walker JN, Flores-Mireles AL, Pinkner CL, Schreiber HLt, Joens MS, Park AM, et al. Catheterization alters bladder ecology to potentiate Staphylococcus aureus infection of the urinary

tract. Proc Natl Acad Sci U S A. 2017;114(41):E8721-E30. Epub 2017/10/05. doi: 10.1073/pnas.1707572114. PubMed PMID: 28973850; PubMed Central PMCID: PMCPMC5642702.

53. Peman J, Ruiz-Gaitan A. Candidemia from urinary tract source: the challenge of candiduria. Hosp Pract (1995). 2018;46(5):243-5. Epub 2018/10/20. doi: 10.1080/21548331.2018.1538623. PubMed PMID: 30334630.

54. Pappas PG, Kauffman CA, Andes DR, Clancy CJ, Marr KA, Ostrosky-Zeichner L, et al. Clinical Practice Guideline for the Management of Candidiasis: 2016 Update by the Infectious Diseases Society of America. Clin Infect Dis. 2016;62(4):e1-50. Epub 2015/12/19. doi: 10.1093/cid/civ933. PubMed PMID: 26679628; PubMed Central PMCID: PMCPMC4725385.

55. Huang PY, Hung MH, Shie SS, Su LH, Chen KY, Ye JJ, et al. Molecular concordance of concurrent Candida albicans candidemia and candiduria. Diagn Micr Infec Dis. 2013;76(3):382-4. doi: 10.1016/j.diagmicrobio.2013.03.015. PubMed PMID: WOS:000321026800026.

56. Kauffman CA, Vazquez JA, Sobel JD, Gallis HA, McKinsey DS, Karchmer AW, et al. Prospective multicenter surveillance study of funguria in hospitalized patients. Clinical Infectious Diseases. 2000;30(1):14-8. doi: Doi 10.1086/313583. PubMed PMID: WOS:000085004800005.

57. Rousseau M, Goh HMS, Holec S, Albert ML, Williams RBH, Ingersoll MA, et al. Bladder catheterization increases susceptibility to infection that can be prevented by prophylactic antibiotic treatment. Jci Insight. 2016;1(15). doi: ARTN e8817810.1172/jci.insight.88178. PubMed PMID: WOS:000387123200009.

58. Conway LJ, Carter EJ, Larson EL. Risk Factors for Nosocomial Bacteremia Secondary to Urinary Catheter-Associated Bacteriuria: A Systematic Review. Urol Nurs. 2015;35(4):191-203. Epub 2015/09/26. PubMed PMID: 26402994; PubMed Central PMCID: PMCPMC4586038.

59. Greene MT, Chang R, Kuhn L, Rogers MA, Chenoweth CE, Shuman E, et al. Predictors of hospital-acquired urinary tract-related bloodstream infection. Infect Control Hosp Epidemiol. 2012;33(10):1001-7. Epub 2012/09/11. doi: 10.1086/667731. PubMed PMID: 22961019; PubMed Central PMCID: PMCPMC3442945.

60. Nicolle LE. Catheter associated urinary tract infections. Antimicrob Resist Infect Control. 2014;3:23. Epub 2014/07/31. doi: 10.1186/2047-2994-3-23. PubMed PMID: 25075308; PubMed Central PMCID: PMCPMC4114799.

61. Rosiana S, Zhang LY, Kim GH, Revtovich AV, Uthayakumar D, Sukumaran A, et al. Comprehensive genetic analysis of adhesin proteins and their role in virulence of Candida albicans. Genetics. 2021;217(2). doi: ARTN iyab00310.1093/genetics/iyab003. PubMed PMID: WOS:000637218100019.

62. Shapiro RS, Chavez A, Porter CBM, Hamblin M, Kaas CS, DiCarlo JE, et al. A CRISPR-Cas9-based gene drive platform for genetic interaction analysis in Candida albicans. Nat Microbiol. 2018;3(1):73-82. Epub 2017/10/25. doi: 10.1038/s41564-017-0043-0. PubMed PMID: 29062088; PubMed Central PMCID: PMCPMC5832965.

63. Noble SM, French S, Kohn LA, Chen V, Johnson AD. Systematic screens of a Candida albicans homozygous deletion library decouple morphogenetic switching and pathogenicity. Nat Genet. 2010;42(7):590-8. Epub 2010/06/15. doi: 10.1038/ng.605. PubMed PMID: 20543849; PubMed Central PMCID: PMCPMC2893244.

64. Rishpana MS, Kabbin JS. Candiduria in Catheter Associated Urinary Tract Infection with Special Reference to Biofilm Production. J Clin Diagn Res. 2015;9(10):DC11-3. Epub 2015/11/12. doi: 10.7860/JCDR/2015/13910.6690. PubMed PMID: 26557518; PubMed Central PMCID: PMCPMC4625237.

65. Keten D, Aktas F, Guzel Tunccan O, Dizbay M, Kalkanci A, Biter G, et al. Catheter-associated urinary tract infections in intensive care units at a university hospital in Turkey. Bosn J Basic Med Sci. 2014;14(4):227-33. Epub 2014/11/28. doi: 10.17305/bjbms.2014.4.140. PubMed PMID: 25428675; PubMed Central PMCID: PMCPMC4333973.

66. Network NHS. Urinary Tract Infection (Catheter-Associated Urinary Tract Infection [CAUTI] and Non-Catheter-Associated Urinary Tract Infection [UTI]) Events Center for Disease Control2021.
67. Tso GHW, Reales-Calderon JA, Tan ASM, Sem X, Le GTT, Tan TG, et al. Experimental evolution of a fungal pathogen into a gut symbiont. Science. 2018;362(6414):589-95. Epub 2018/11/06. doi: 10.1126/science.aat0537. PubMed PMID: 30385579.
68. Witchley JN, Penumetcha P, Abon NV, Woolford CA, Mitchell AP, Noble SM. Candida albicans Morphogenesis Programs Control the Balance between Gut Commensalism and Invasive Infection. Cell Host Microbe. 2019;25(3):432-43 e6. Epub 2019/03/15. doi: 10.1016/j.chom.2019.02.008. PubMed PMID: 30870623; PubMed Central PMCID: PMCPMC6581065.
69. Yan L, Yang C, Tang J. Disruption of the intestinal mucosal barrier in Candida albicans infections. Microbiol Res. 2013;168(7):389-95. Epub 2013/04/03. doi: 10.1016/j.micres.2013.02.008. PubMed PMID: 23545353.
70. Glahn BE, Braendstrup O, Olesen HP. Influence of drainage conditions on mucosal bladder damage by indwelling catheters. II. Histological study. Scand J Urol Nephrol. 1988;22(2):93-9. Epub 1988/01/01. doi: 10.1080/00365599.1988.11690392. PubMed PMID: 3206221.
71. Kojic EM, Darouiche RO. Candida infections of medical devices. Clin Microbiol Rev. 2004;17(2):255-67. Epub 2004/04/16. doi: 10.1128/cmr.17.2.255-267.2004. PubMed PMID: 15084500; PubMed Central PMCID: PMCPMC387407.
72. Azmy M, Nawar N, Mohiedden M, Warille L. Electron Microscopic Assay of Bacterial Biofilm Formed on Indwelling Urethral Catheters. Journal of the Egyptian Society of Parasitology. 2016;46(3):475-84. PubMed PMID: 30230743.
73. Wheeler ML, Limon JJ, Underhill DM. Immunity to Commensal Fungi: Detente and Disease. Annu Rev Pathol. 2017;12:359-85. Epub 2017/01/10. doi: 10.1146/annurev-pathol-052016-100342. PubMed PMID: 28068483; PubMed Central PMCID: PMCPMC6573037.
74. Iliev ID, Underhill DM. Striking a balance: fungal commensalism versus pathogenesis. Curr Opin Microbiol. 2013;16(3):366-73. Epub 2013/06/13. doi: 10.1016/j.mib.2013.05.004. PubMed PMID: 23756050; PubMed Central PMCID: PMCPMC3742553.
75. Desai JV, Lionakis MS. The role of neutrophils in host defense against invasive fungal infections. Curr Clin Microbiol Rep. 2018;5(3):181-9. Epub 2019/09/26. doi: 10.1007/s40588-018-0098-6. PubMed PMID: 31552161; PubMed Central PMCID: PMCPMC6758935.
76. Kenno S, Perito S, Mosci P, Vecchiarelli A, Monari C. Autophagy and Reactive Oxygen Species Are Involved in Neutrophil Extracellular Traps Release Induced by C. albicans Morphotypes. Front Microbiol. 2016;7:879. Epub 2016/07/05. doi: 10.3389/fmicb.2016.00879. PubMed PMID: 27375599; PubMed Central PMCID: PMCPMC4896927.
77. Hoyer LL, Cota E. Candida albicans Agglutinin-Like Sequence (Als) Family Vignettes: A Review of Als Protein Structure and Function. Front Microbiol. 2016;7:280. Epub 2016/03/26. doi: 10.3389/fmicb.2016.00280. PubMed PMID: 27014205; PubMed Central PMCID: PMCPMC4791367.
78. Salgado PS, Yan R, Taylor JD, Burchell L, Jones R, Hoyer LL, et al. Structural basis for the broad specificity to host-cell ligands by the pathogenic fungus Candida albicans. Proc Natl Acad Sci U S A. 2011;108(38):15775-9. Epub 2011/09/08. doi: 10.1073/pnas.1103496108. PubMed PMID: 21896717; PubMed Central PMCID: PMCPMC3179088.
79. Lin J, Oh SH, Jones R, Garnett JA, Salgado PS, Rusnakova S, et al. The peptide-binding cavity is essential for Als3-mediated adhesion of Candida albicans to human cells. J Biol Chem. 2014;289(26):18401-12. Epub 2014/05/08. doi: 10.1074/jbc.M114.547877. PubMed PMID: 24802757; PubMed Central PMCID: PMCPMC4140257.
80. Glazier VE. EFG1, Everyone's Favorite Gene in Candida albicans: A Comprehensive Literature Review. Frontiers in Cellular and Infection Microbiology. 2022;12. doi: 10.3389/fcimb.2022.855229.

81. Cavalheiro M, Teixeira MC. Candida Biofilms: Threats, Challenges, and Promising Strategies. Front Med (Lausanne). 2018;5:28. Epub 2018/03/01. doi: 10.3389/fmed.2018.00028. PubMed PMID: 29487851; PubMed Central PMCID: PMCPMC5816785.

82. Schindelin J, Arganda-Carreras I, Frise E, Kaynig V, Longair M, Pietzsch T, et al. Fiji: an open-source platform for biological-image analysis. Nat Methods. 2012;9(7):676-82. Epub 2012/06/30. doi: 10.1038/nmeth.2019. PubMed PMID: 22743772; PubMed Central PMCID: PMCPMC3855844.

Acknowledgments We thank members of the A.L.F.M. and F.H.S.T. laboratories for their helpful suggestions and insightful comments. Special thank you to Dr. Michael G. Caparon for his comments. Special thank you to Dr. Sara Cole and the ND Integrated Imaging Facility for tissue processing and support during imaging. **Funding:** This work was supported by institutional funds from the University of Notre Dame (to A.L.F.M. and F.H.S.T), National Institute of Health grant R01-DK128805 (to A.L.F.M., and M.J.A.), Arthur J. Schmitt Leadership Fellowship (A.A.L.), and CIFAR Azrieli Global Scholar Award and Canadian Institutes of Health Research (CIHR) Project Grant PJT162195 (to R.S.S). **Author contributions** A.L.F.M., and F.H.S.T designed the experiments. A.A.L., M.J.A., A.M., J.J.M., and P.S. performed the studies. R.S.S. and N.C.G. designed and generated the adhesin mutant strain collection and the *ALS1* OE strain. A.A.L., A.L.F.M, and F.H.S.T. wrote the paper.

Competing interests: The authors declare no competing financial interests.

Figures:

Figure 1. *C. albicans* grows, survives, and switches to hyphal morphology when grown in urine. (A-F) Growth curves of *C. albicans* Pt62 (A), Pt65 (B), PCNL1 (C), DAY230 (D), SC5314 (E), and SC5314 *efg1*Δ*cph1*Δ (F), grown in human urine conditions alone, or urine conditions supplemented with 3% human serum (serum), fibrinogen (Fg), bovine serum albumin (BSA), or amino acids (AA). Fungal growth was determined by CFUs enumeration after 0, 24, and 48 hours. Except when indicated, all strains were grown under static conditions. Data presented shows the mean and standard error of the mean derived from three independent experiments with at least three technical replicates. **(G-M)** The morphology of *C. albicans* strains were evaluated after 0, 24, and 48 hours of growth in urine and YPD with or without 3% human serum. Images (consisting of a 3 x 3 tiled region, i.e. 9 fields of view) were randomly acquired and at least three images were analyzed per condition. The total number of cells per phenotype were summed and divided by the total number of cells to give the overall percentage of yeast, pseudohyphae, and hyphae (**M**). Differences between groups were tested for significance using the Mann-Whitney U test. *, $P < 0.05$; **, $P < 0.005$; ***, $P < 0.0005$; and ****, $P < 0.0001$. P-value colors represent the comparison between the different populations: hyphae (red), pseudohyphae (orange), and yeast (black).

Figure 2. Fibrinogen/fibrin interaction with *C. albicans* enhances biofilm formation. (**A-F**) Immunostaining analysis of biofilm formation on BSA- or Fg- coated microplates by *C. albicans* strains when grown in YPD, BHI, or human urine. At 48 hrs, *C. albicans'* biofilm was measured via fluorescence intensity by using anti-*Candida* antibodies. Data presented shows the mean and standard error derived from three independent experiments with 24 technical replicates.

Differences between groups were tested for significance using the Mann-Whitney U test. ****, P<0.0001; ns, not statistically different. (**G-L**) Microscopic visualization of 48 hrs *C. albicans'* biofilms biomass on BSA- or Fg-coated glass bottom petri dishes grown in urine using anti-*Candida* antibodies. White squares represent the zoom-in area used for the higher magnification (x). (**M-R**) Microscopic visualization and 3D reconstruction of 48 hrs *C. albicans'* biofilms on fibrin fibers/meshes grown in human urine using antibodies against Fg (anti-Fg; green) and *C. albicans* (anti–Candida; red). Scale bars: 50 µm.

Figure 3. Urinary catheterization promotes fungal colonization and hyphal formation is required for CAUTI. (**A-D**) Fungal burden of clinical and lab strains on the harvested organs and catheter. (**E**) Fungal burden comparison between SC5314 WT and SC5314 *efg1*Δ*cph1*Δ strains. Values represent means ± SEM. The Mann-Whitney U test was used; *, $P < 0.05$ was considered statistically significant. **, $P < 0.005$; ns, values were not statistically significantly different. The horizontal bar represents the median value. The horizontal broken line represents the limit of detection of viable fungi. LOD; limit of detection. Animals that lost the catheter were not included in this work.

Figure 4. Hyphal *C. albicans* cells invade the lumen of the catheterized bladder and interact with fibrinogen on the bladders and catheters. (**A-F**) Implanted and infected bladders and catheters were recovered at 24hpi. Bladders were subjected to analysis by H&E and IF staining. For the IF analysis antibody staining was used to detect Fg (anti-Fg; green), *C. albicans* (anti–*Candida*; red), and neutrophils (anti-Ly6G; white). Antibody staining with DAPI (blue) delineated the urothelium and cell nuclei (representative images). The white broken line

separates the bladder lumen (L) from the urothelium surface (U), the lamina propria (LP), and muscularis (M). H&E stained bladder scale bars, 700 µm. White squares represent a zoom-in for the next magnification (x). Blue arrow heads indicate *C. albicans* colonization. (**G-M**) Implanted catheters were stained with antibodies to detect Fg (anti-Fg; green) and *C. albicans* (anti-Candida; red). (**N-R**) Quantification of fungal colocalization with deposited Fg on the catheter. The Mann-Whitney U test was used to analyze catheter colonization between SC5314 WT and hyphal mutant; *, $P < 0.05$; Values represent the means ± standard deviation derived from co-localization of the catheter segments. Non-implanted catheters were used a negative control (**G**).

Figure 5. Efg1 is responsible for inducing hyphal morphology and is critical for establishment of CAUTI. (**A**) Comparison of biofilm formation on Fg-coated microplates by *C. albicans* strains when grown in urine for 48 hours. (**B**) Microscopic visualization and 3D reconstruction of *C. albicans*-fibrin/meshes interaction grown in urine using antibodies against Fg (anti-Fg; green) and *C. albicans* (anti-*Candida*; red). Scale bars: 50 µm for 40x. (**C**) Mice were catheterized and challenged with $1x10^6$ CFU of each strain, and burdens in organs or catheters were quantitated as the number of CFUs recovered. (**D**) Mouse bladders were harvested following infection and catheter implantation. Bladders were subjected to analysis by H&E and IF staining (anti-Fg, green; anti-*Candida*, red; anti-Ly6G, white; DAPI, blue). Values represent means ± SEM. The Mann-Whitney U test was used; $P < 0.05$ was considered statistically significant. *, $P < 0.05$; **, $P < 0.005$; ***, $P < 0.0005$. The horizontal bar represents the median value. The horizontal broken line represents the limit of detection of viable fungi. Animals that lost the catheter were not included in this work.

Figure 6. Als1 is critical for Fg-dependent biofilm formation and establishment of CAUTI. Biofilm formation analysis on Fg- coated microplates by *C. albicans* adhesin mutant strains (**A**) or *ALS1* OE strain (**B**) when grown in human urine. At 48 hrs, *C. albicans'* biofilm was measured via fluorescence intensity by using anti-*Candida* antibodies (**A**) or crystal violet (**B**). (**A-B**) Data presented shows the mean and standard error derived from three independent experiments with 24 technical replicates. (**C**) Microscopic visualization and 3D reconstruction of *C. albicans*-fibrin/meshes interaction grown in urine using antibodies against Fg (green) and *C. albicans* (red). Scale bars: 50 µm for 40x. (**D**) Fungal burden in organs or catheters at 24 hpi were quantitated as the number of CFUs recovered. (**E**) H&E and IF analysis of catheterized and infected bladder. IF staining was performed to detect Fg (green), *C. albicans* (red), and neutrophils (white). DAPI (blue) was used to stain the cell nuclei and delineated the urothelium (representative images). L, represents; U, urothelium; LP, the lamina propria; and M, muscularis. Bladder scale bars, 700 µm. White squares represent a zoom-in for the next magnification (x). Blue arrow heads on H&E indicate *C. albicans* bladder colonization. (**F**) *C. albicans* and Fg colocalization in implanted catheters using antibodies against Fg (anti-Fg; green) and *C. albicans* (anti-Candida; red). (**G**) Quantification of fungal colocalization with deposited Fg on the catheter. For biofilm formation, fungal burden and colocalization analysis values represent means ± SEM. The Mann-Whitney U test was used; *, $P < 0.05$; **, $P < 0.005$; ***, $P < 0.0005$; and ****, $P < 0.0001$. The horizontal bar represents the median value. (**D**) The horizontal broken line represents the limit of detection of viable fungi. Animals that lost the catheter were not included in this work.

Figure 7. *C. albicans* hyphal morphology and Als1-Fg interaction are critical for CAUTI. Urinary catheterization results in mechanical damage to the bladder and leads to the release of Fg, accumulating in the bladder and depositing on the urinary catheter. The Fg-coated catheter serves as a scaffold for *C. albicans* attachment, leading to robust biofilm formation consisting of yeast, pseudohyphae, and hyphae. *C. albicans'* attachment to Fg can be attributed primarily to the adhesin Als1. As a result of this adherence to Fg, *C. albicans* is able to persist in the bladder and establish CAUTI.

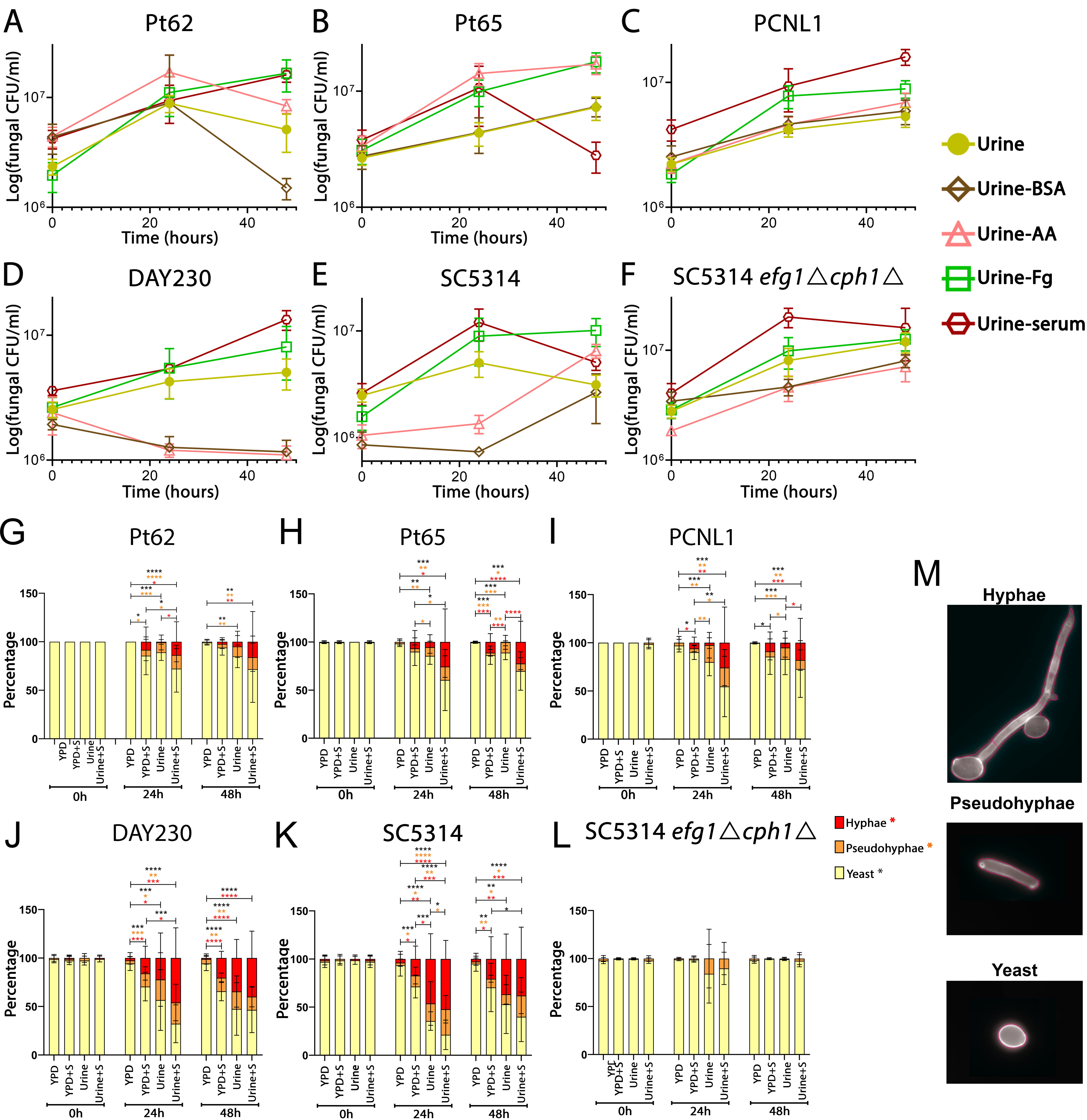
A
Pt62
B
Pt65
C
PCNL1
D
DAY230
E
SC5314
F
SC5314 efg1△cph1△
Log(fungal CFU/ml)
10^6
10^7
0
20
40
Time (hours)
Urine
Urine-BSA
Urine-AA
Urine-Fg
Urine-serum
G
Pt62
H
Pt65
I
PCNL1
J
DAY230
K
SC5314
L
SC5314 efg1△cph1△
Percentage
0
50
100
150
YPD
YPD+S
Urine
Urine+S
0h
24h
48h
Hyphae *
Pseudohyphae *
Yeast *
M
Hyphae
Pseudohyphae
Yeast

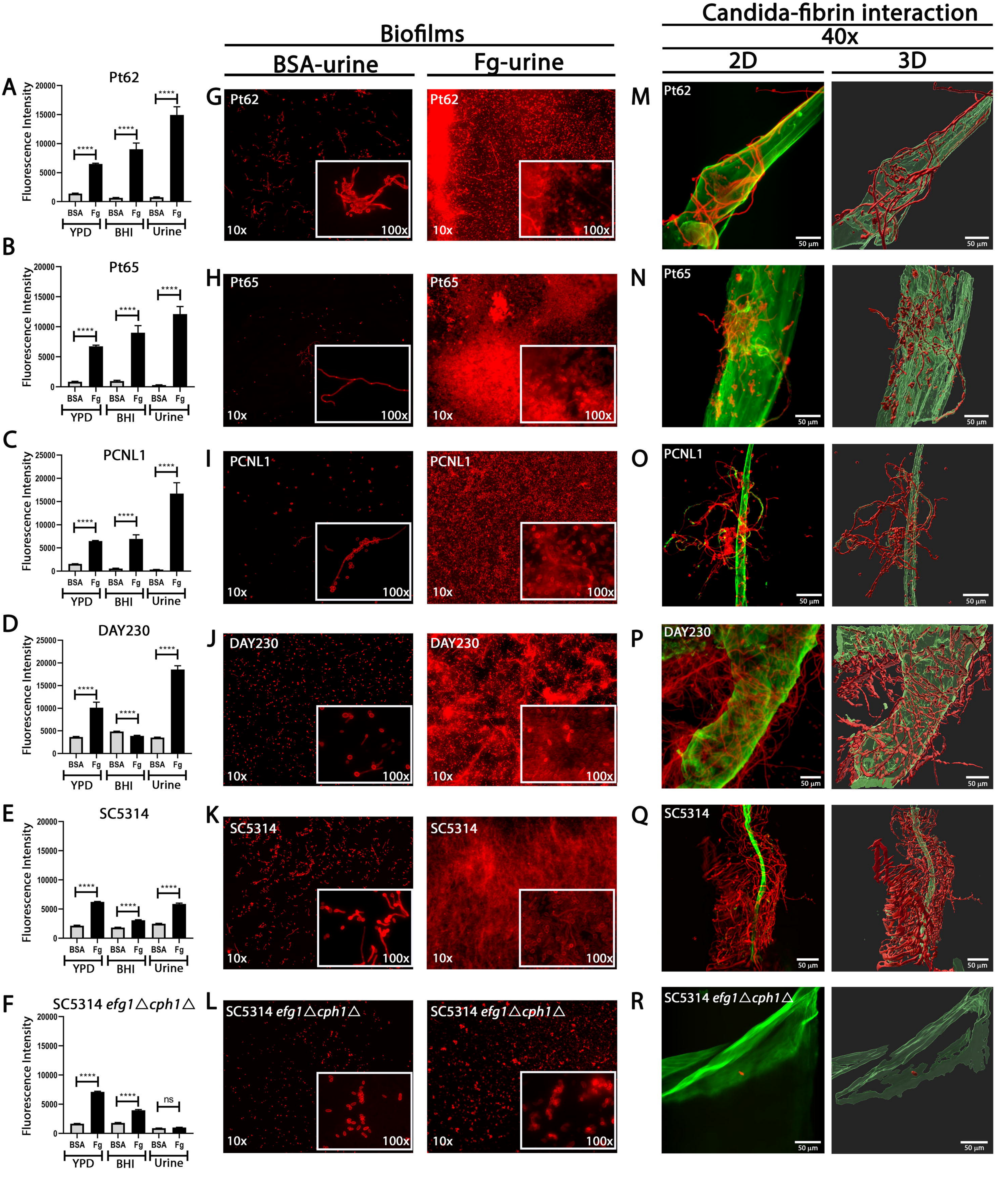
Biofilms
BSA-urine
Fg-urine
Candida-fibrin interaction
40x
2D
3D
A
Pt62
Fluorescence Intensity
20000
15000
10000
5000
0
BSA Fg BSA Fg BSA Fg
YPD BHI Urine
****
B
Pt65
C
PCNL1
25000
D
DAY230
E
SC5314
F
SC5314 efg1△cph1△
ns
G
H
I
J
K
L
M
N
O
P
Q
R
10x
100x
50 µm

A
Pt62
B
Pt65
C
PCNL1
D
DAY230
E
SC5314
log(fungal CFU/org or catheter)
10^1
10^2
10^3
10^4
10^5
10^6
10^7
LOD
**
*
Bladder
Kidney
Spleen
Heart
Catheter
WT
efg1Δcph1Δ
Non-catheterized
Catheterized

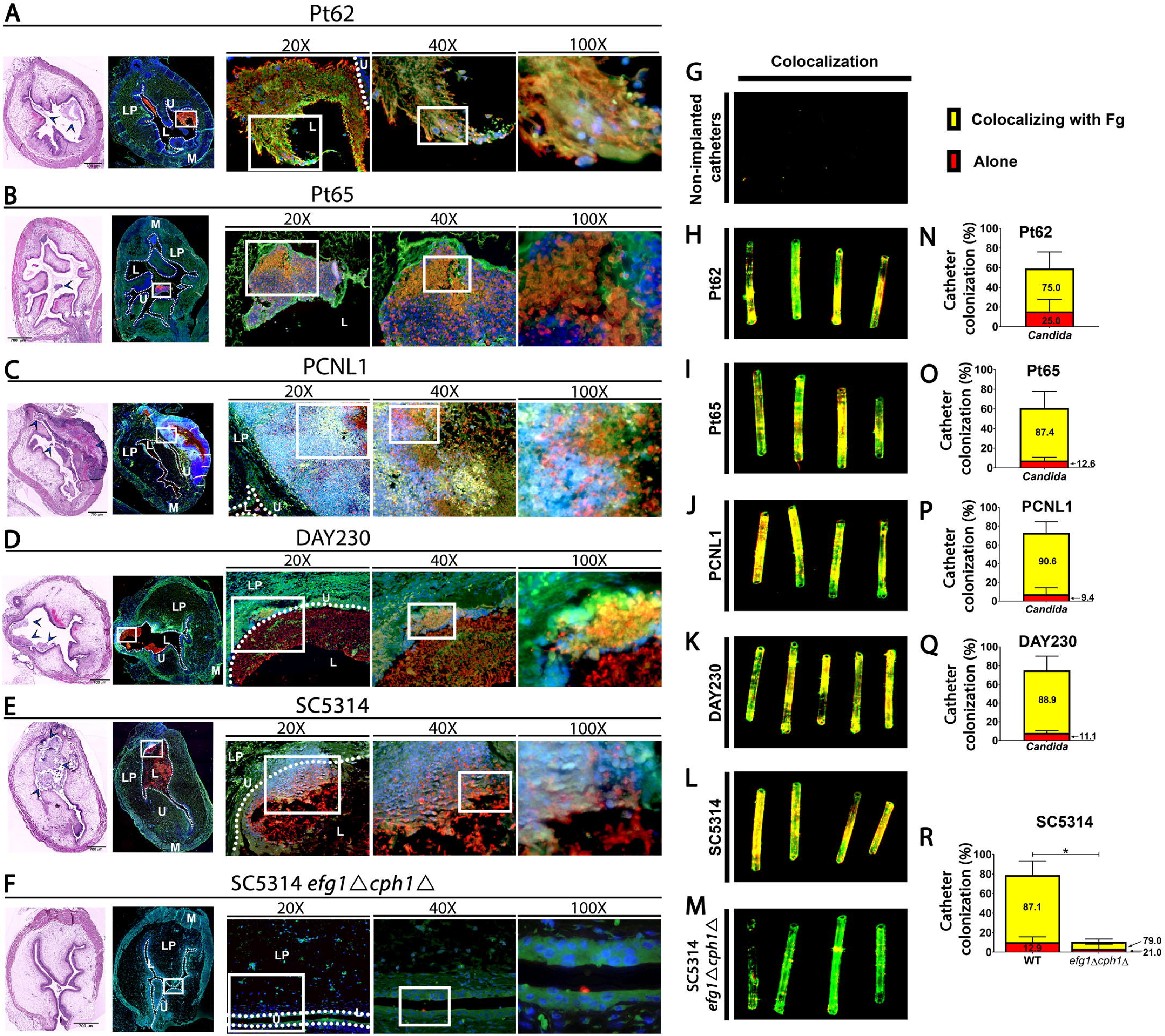
A
Pt62
20X
40X
100X
LP
U
L
M
B
Pt65
C
PCNL1
D
DAY230
E
SC5314
F
SC5314 efg1△cph1△
700 μm
Colocalization
G
Non-implanted catheters
Colocalizing with Fg
Alone
H
Pt62
I
Pt65
J
PCNL1
K
DAY230
L
SC5314
M
SC5314 efg1△cph1△
N
Pt62
Catheter colonization (%)
0
20
40
60
80
100
75.0
25.0
Candida
O
Pt65
87.4
12.6
Candida
P
PCNL1
90.6
9.4
Candida
Q
DAY230
88.9
11.1
Candida
R
SC5314
*
87.1
12.9
79.0
21.0
WT
efg1△cph1△

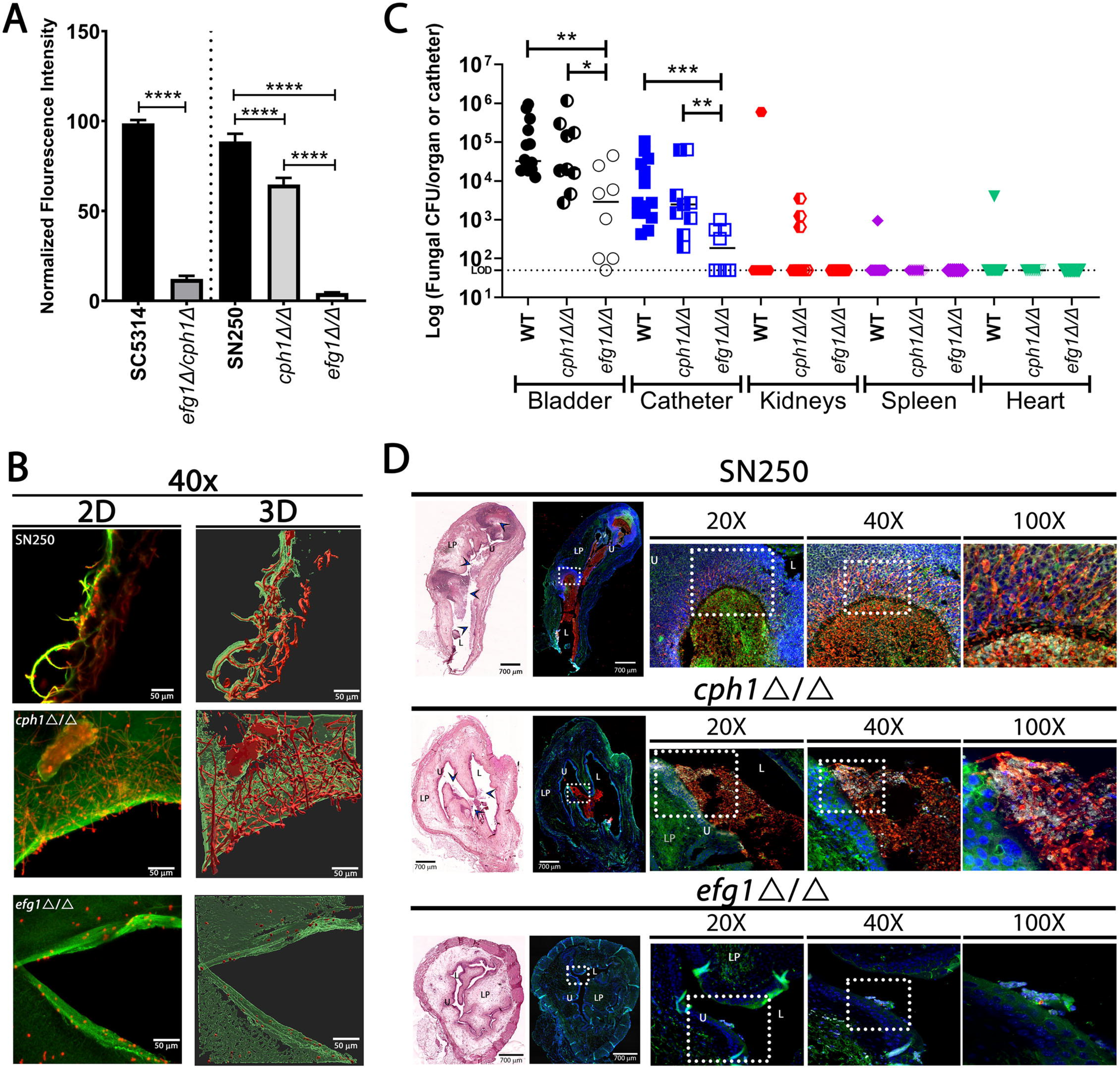
A
Normalized Flourescence Intensity
150
100
50
0
****
****
****
****
SC5314
efg1Δ/cph1Δ
SN250
cph1Δ/Δ
efg1Δ/Δ
C
Log (Fungal CFU/organ or catheter)
10^7
10^6
10^5
10^4
10^3
10^2
LOD
10^1
**
*
***
**
WT
cph1Δ/Δ
efg1Δ/Δ
Bladder
Catheter
Kidneys
Spleen
Heart
B
40x
2D
3D
SN250
cph1△/△
efg1△/△
50 µm
D
SN250
cph1△/△
efg1△/△
20X
40X
100X
LP
U
L
700 µm

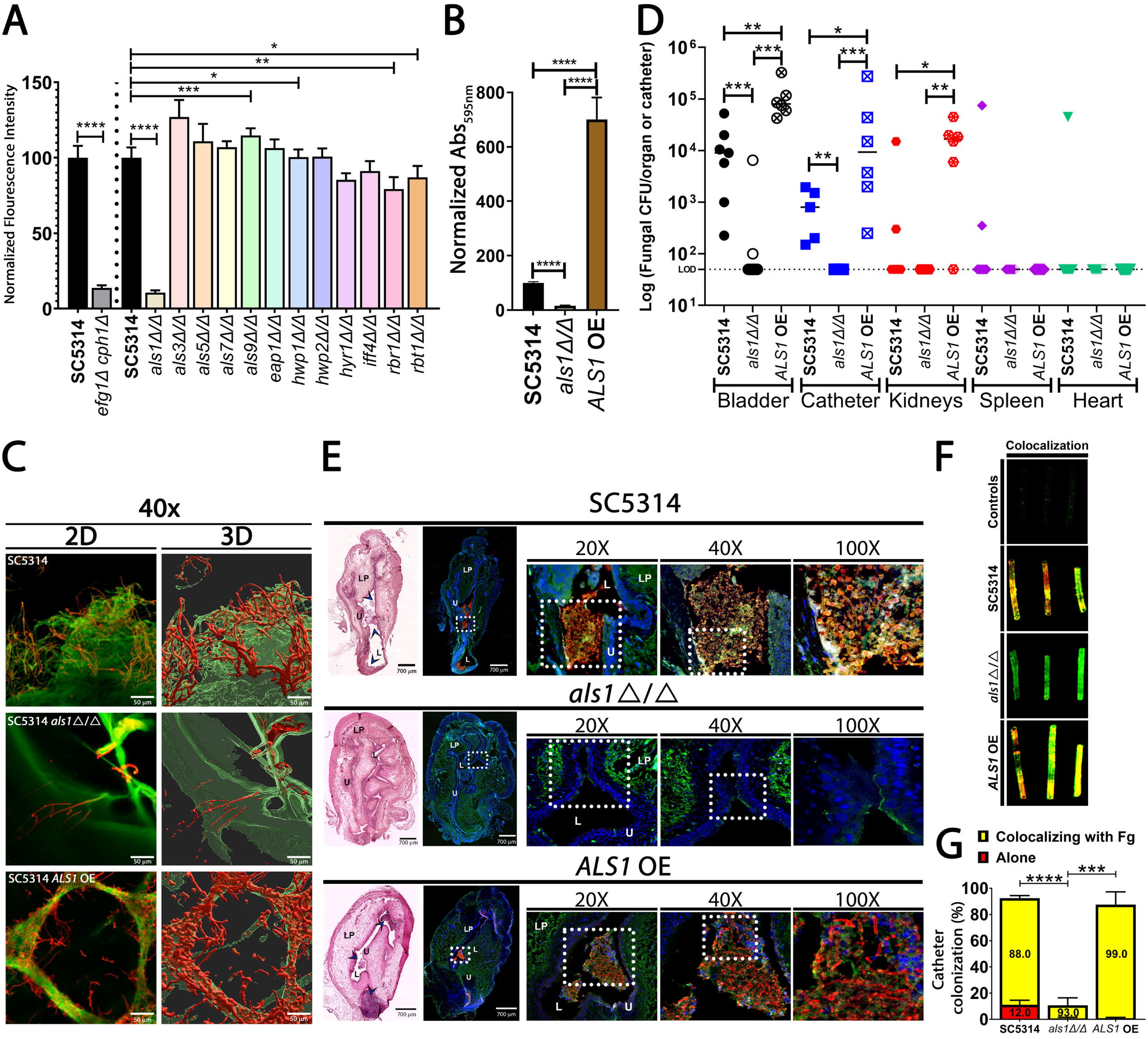

A
Normalized Flourescence Intensity
150
100
50
0
SC5314
efg1Δ cph1Δ
SC5314
als1Δ/Δ
als3Δ/Δ
als5Δ/Δ
als7Δ/Δ
als9Δ/Δ
eap1Δ/Δ
hwp1Δ/Δ
hwp2Δ/Δ
hyr1Δ/Δ
iff4Δ/Δ
rbr1Δ/Δ
rbt1Δ/Δ
****
****
***
*
**
*
B
Normalized Abs$_{595nm}$
800
600
400
200
0
SC5314
als1Δ/Δ
ALS1 OE
****
****
****
D
Log (Fungal CFU/organ or catheter)
10^6
10^5
10^4
10^3
10^2
LOD
10^1
SC5314
als1Δ/Δ
ALS1 OE
Bladder
Catheter
Kidneys
Spleen
Heart
**
***
***
*
***
**
*
**
C
40x
2D
3D
SC5314
SC5314 als1△/△
SC5314 ALS1 OE
50 µm
E
SC5314
als1△/△
ALS1 OE
20X
40X
100X
LP
U
L
700 µm
F
Colocalization
Controls
SC5314
als1△/△
ALS1 OE
G
Colocalizing with Fg
Alone
Catheter colonization (%)
100
80
60
40
20
0
88.0
12.0
93.0
99.0
SC5314
als1Δ/Δ
ALS1 OE
****
***

ALS1
Candida Yeast
Candida Hyphae
Fibrinogen